Compound	1	7
Optimized Structures	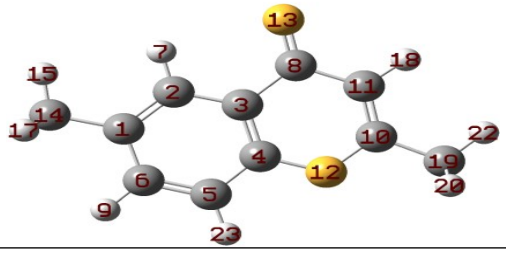	
LUMO	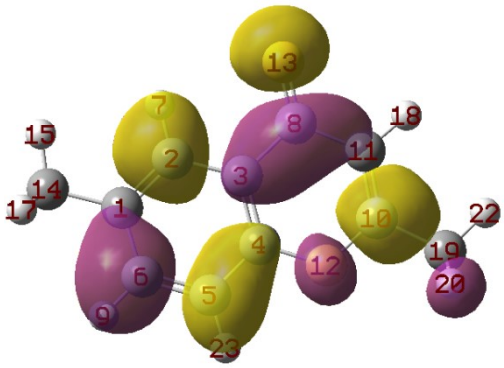 E_{LUMO} = -1.761	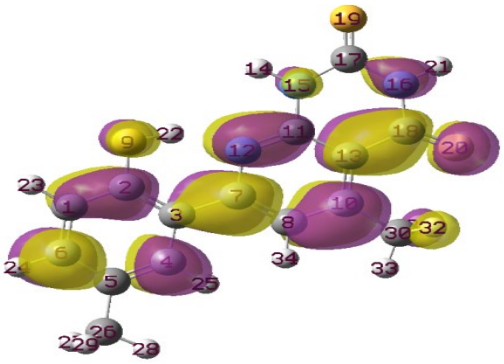 E_{LUMO} = **-2.365**
HOMO	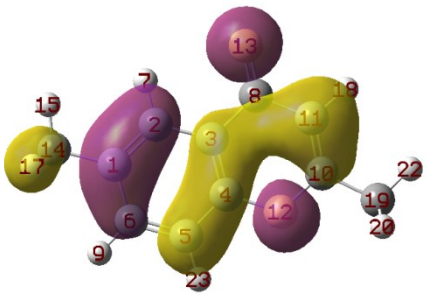 E_{HOMO}= **-6.655**	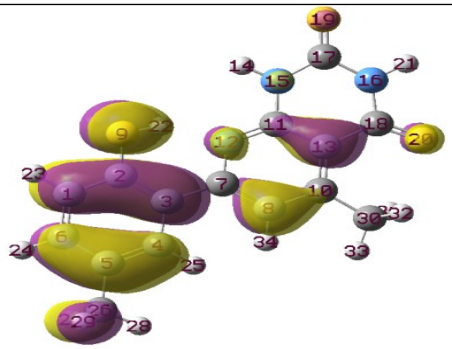 E_{HOMO}= **-6.096**

Fig. S1. Molecular modeling and the electron density of HOMO and LUMO of compounds **1** and **7**

Compound	8	9
Optimized Structures	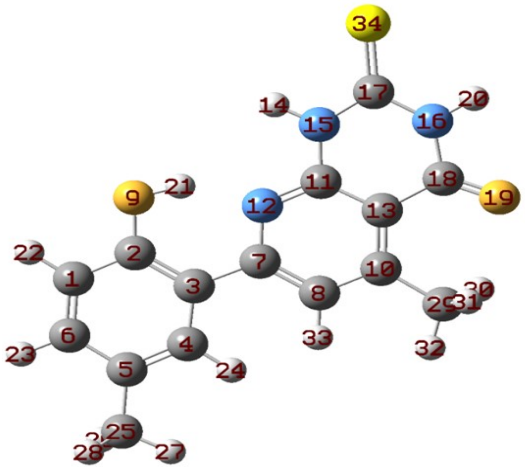	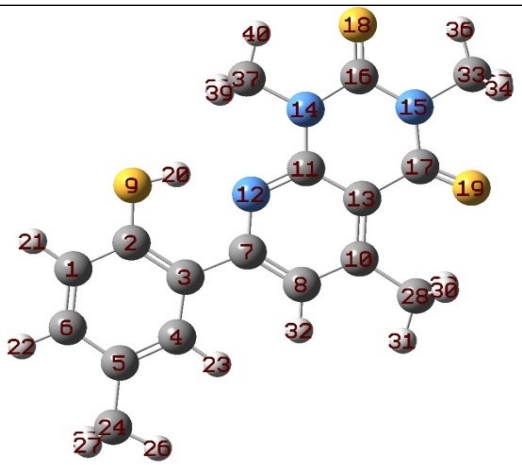
LUMO	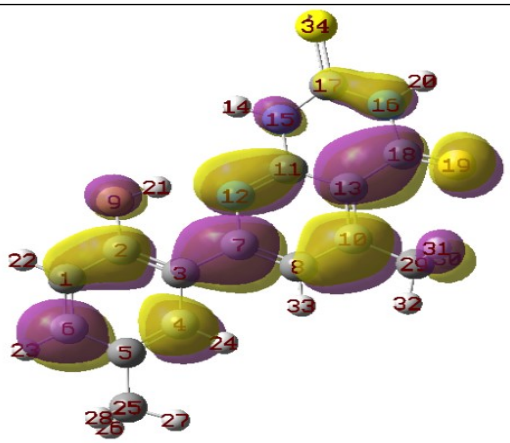 E_{LUMO} = -2.535	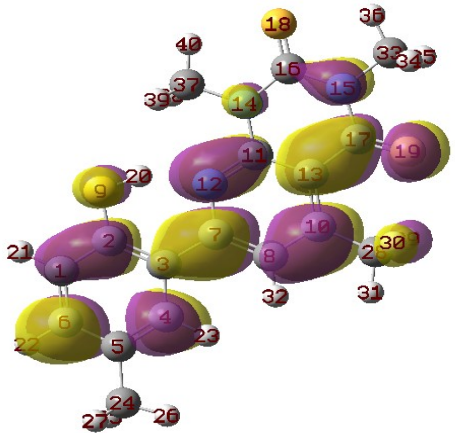 E_{LUMO} = -2.229
HOMO	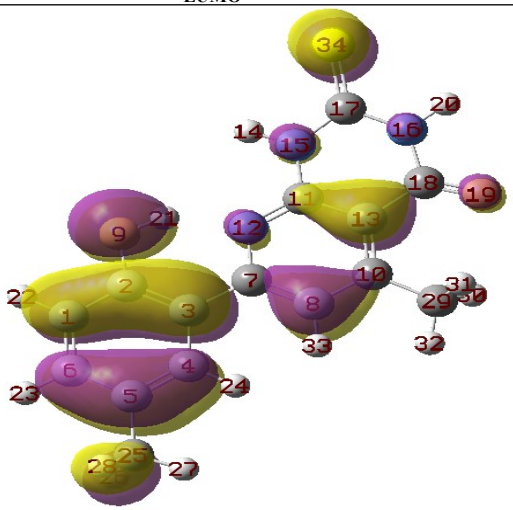 E_{HOMO}= -6.192	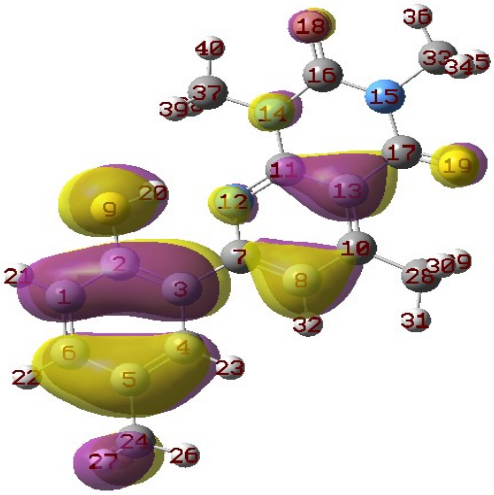 E_{HOMO}= -5.998

Fig. S2. Molecular modeling and the electron density of HOMO and LUMO of compounds **8** and **9**

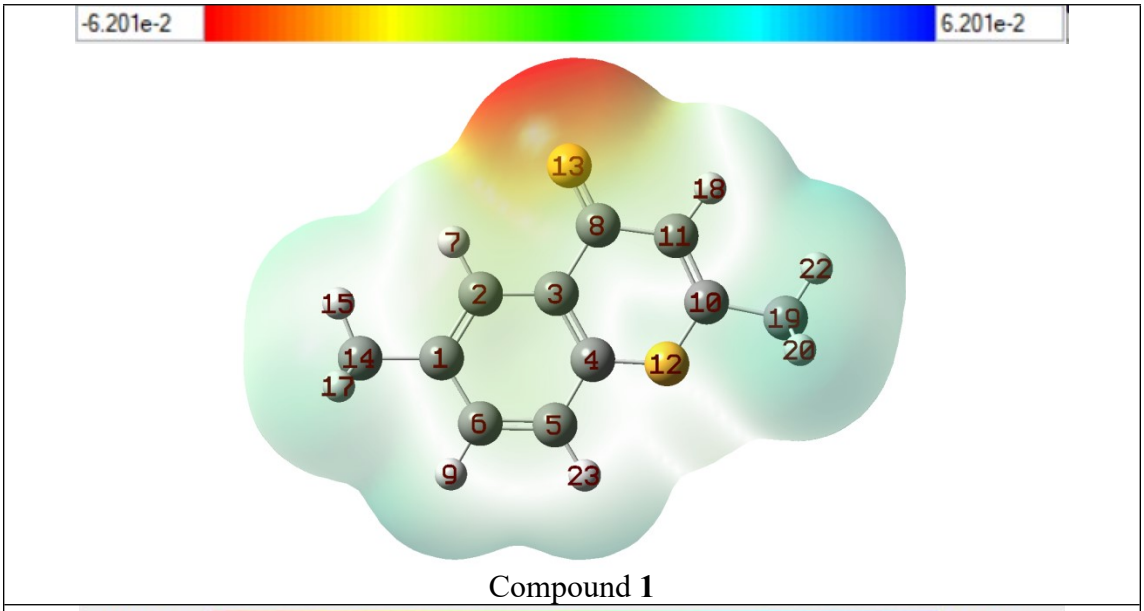

Compound **1**

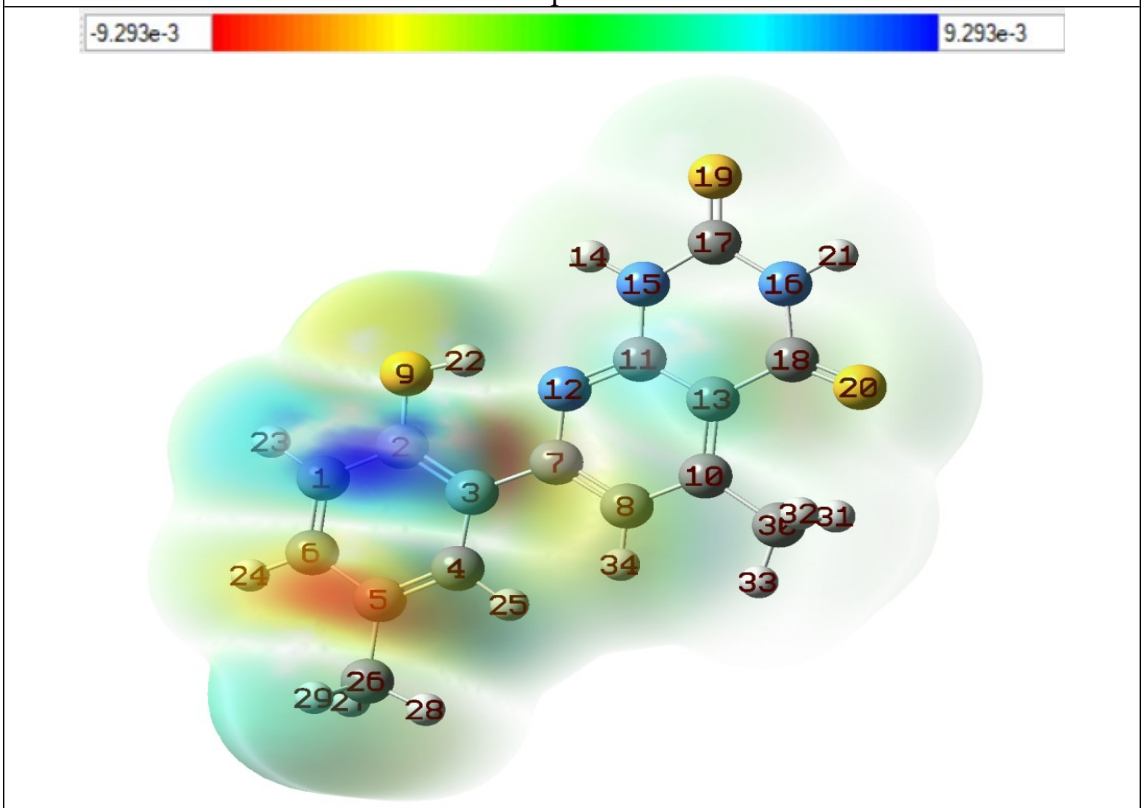

Compound **7**

Fig. S3. Molecular electrostatic potential of compounds **1** and **7**

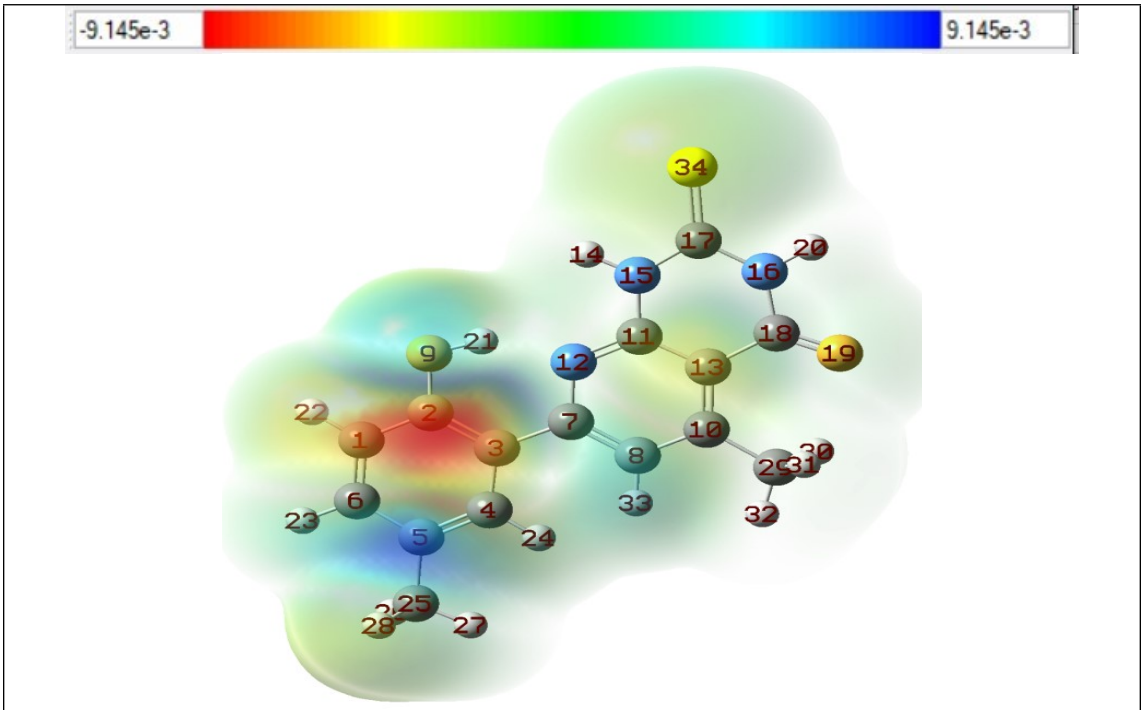

Compound **8**

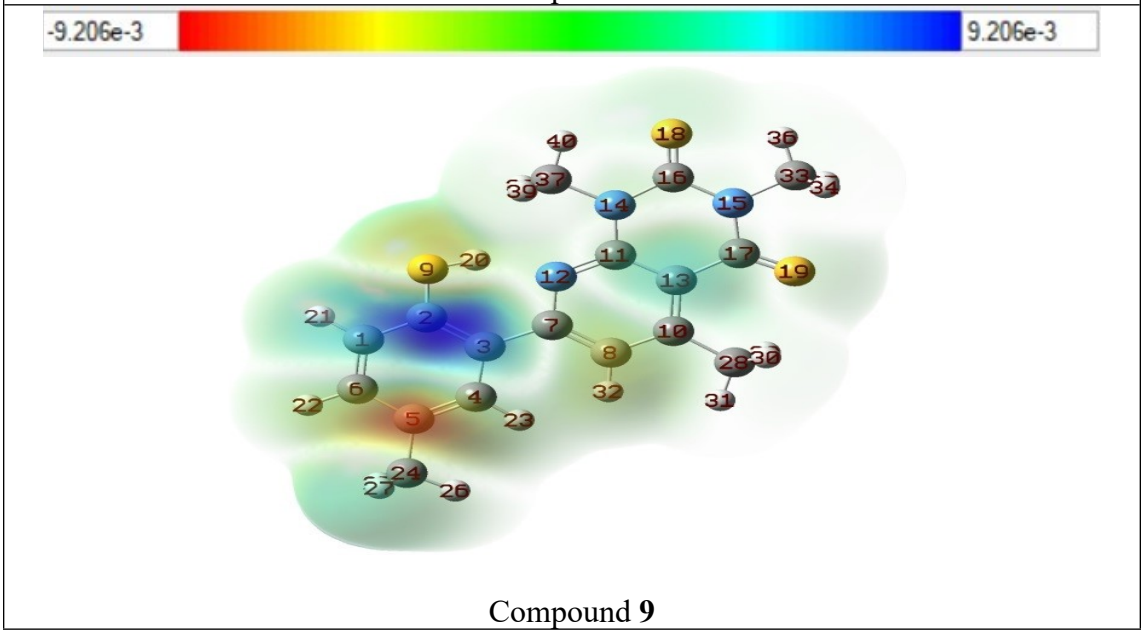

Compound **9**

Fig. S4. Molecular electrostatic potential of compounds **8** and **9**

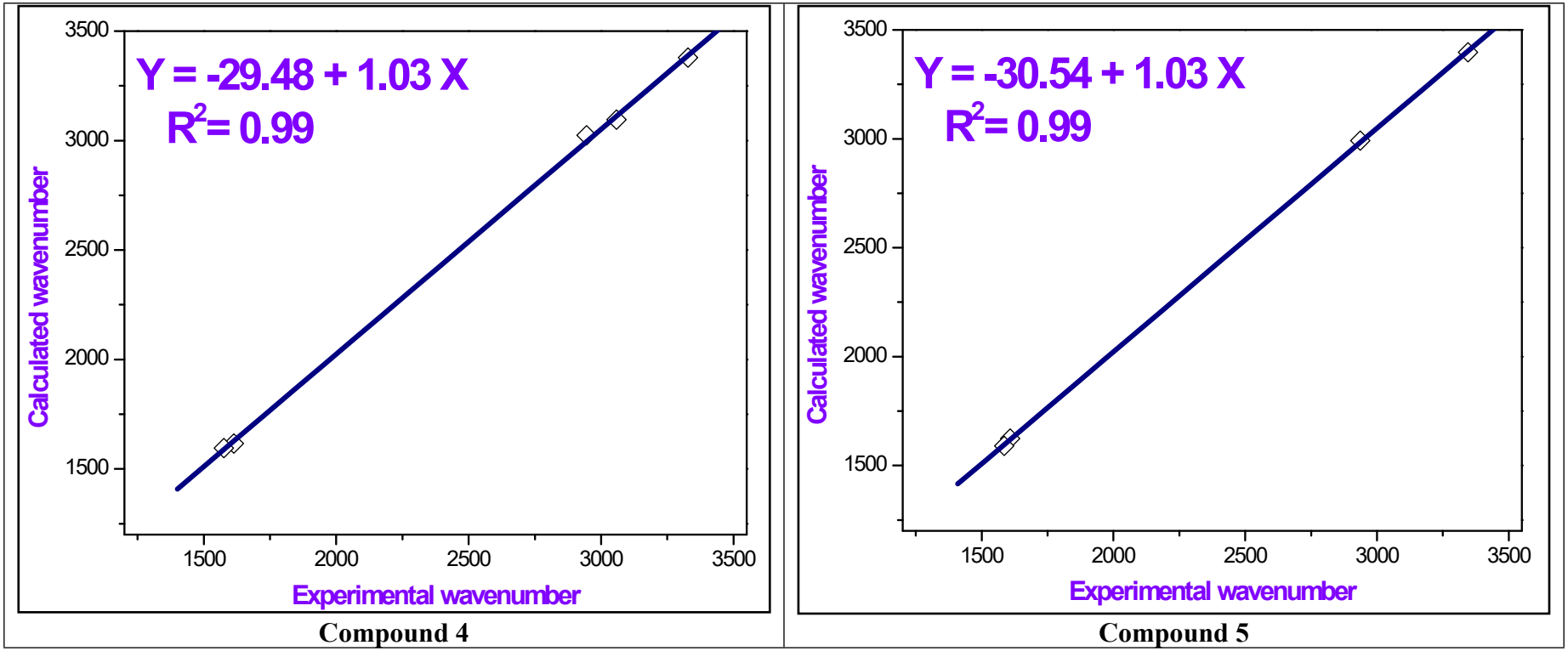

Fig. S5. The correlation relationships of the experimental *versus* calculated IR wavenumbers of compounds **4** and **5**.

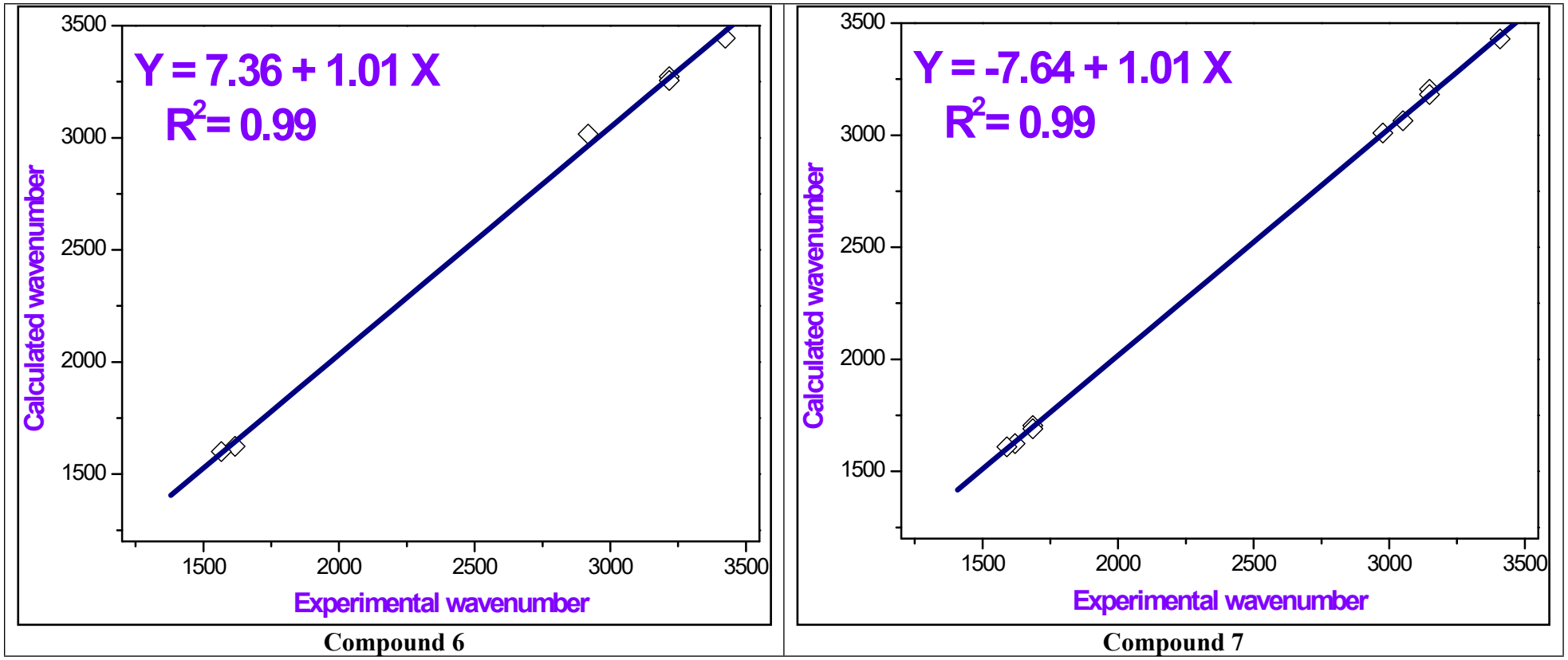

Fig. S6. The correlation relationships of the experimental *versus* calculated IR wavenumbers of compounds **6** and **7**.

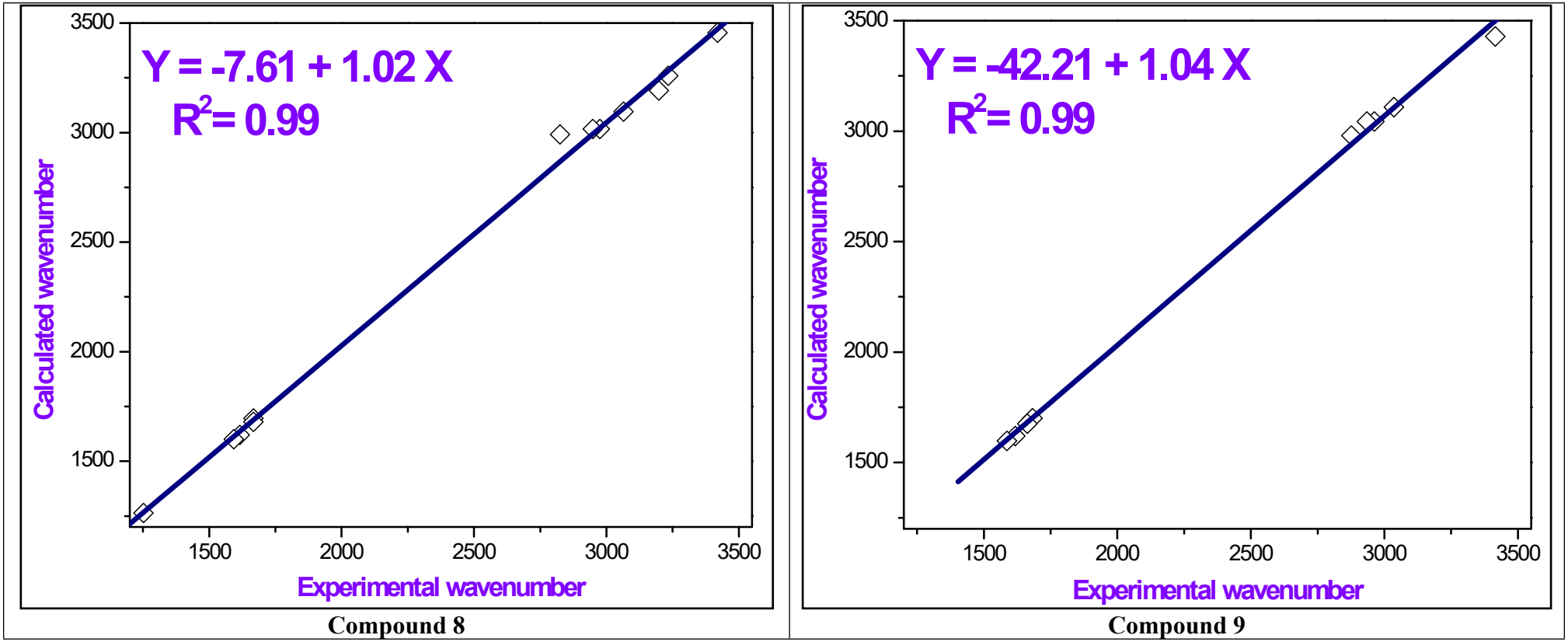

Fig. S7. The correlation relationships of the experimental *versus* calculated IR wavenumbers of compounds **8** and **9**.

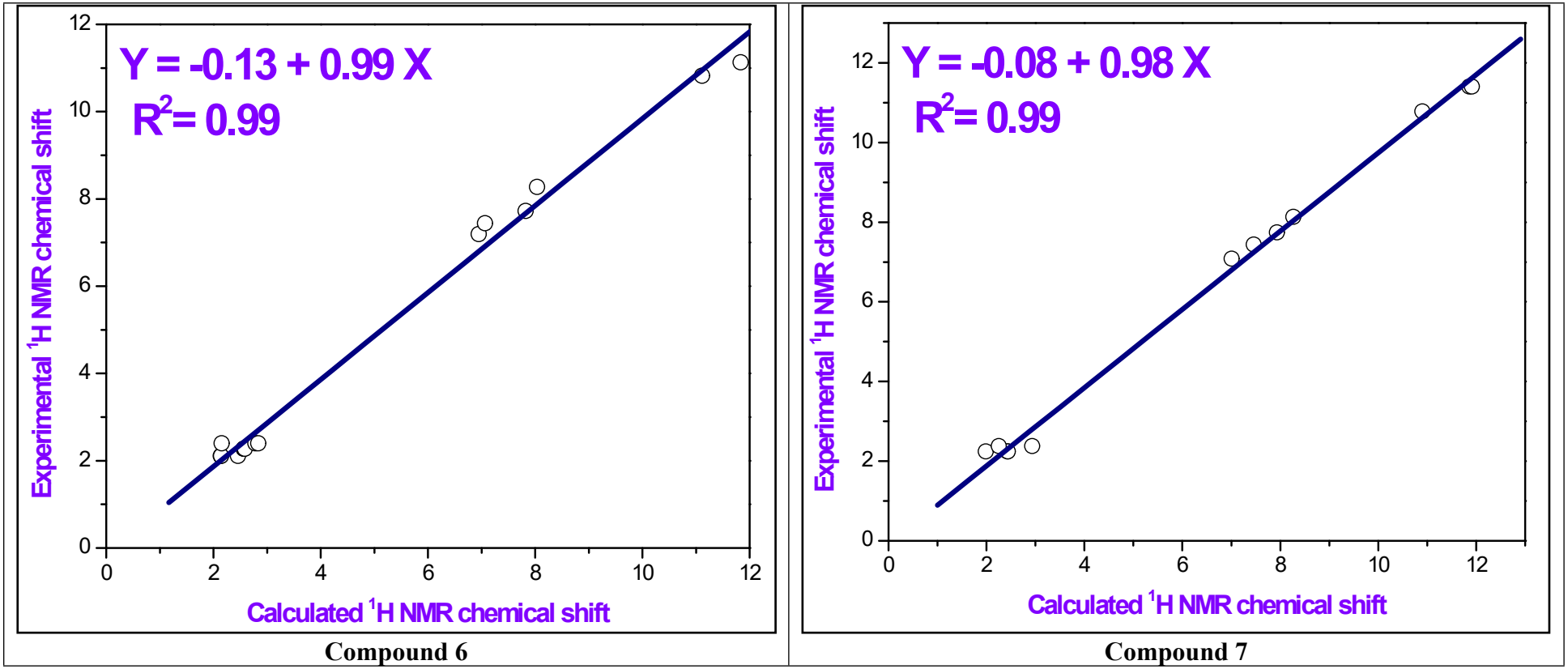

Fig. S8. The correlation relationships of the experimental *versus* calculated ^{1}H NMR chemical shifts of compounds **6** and **7**.

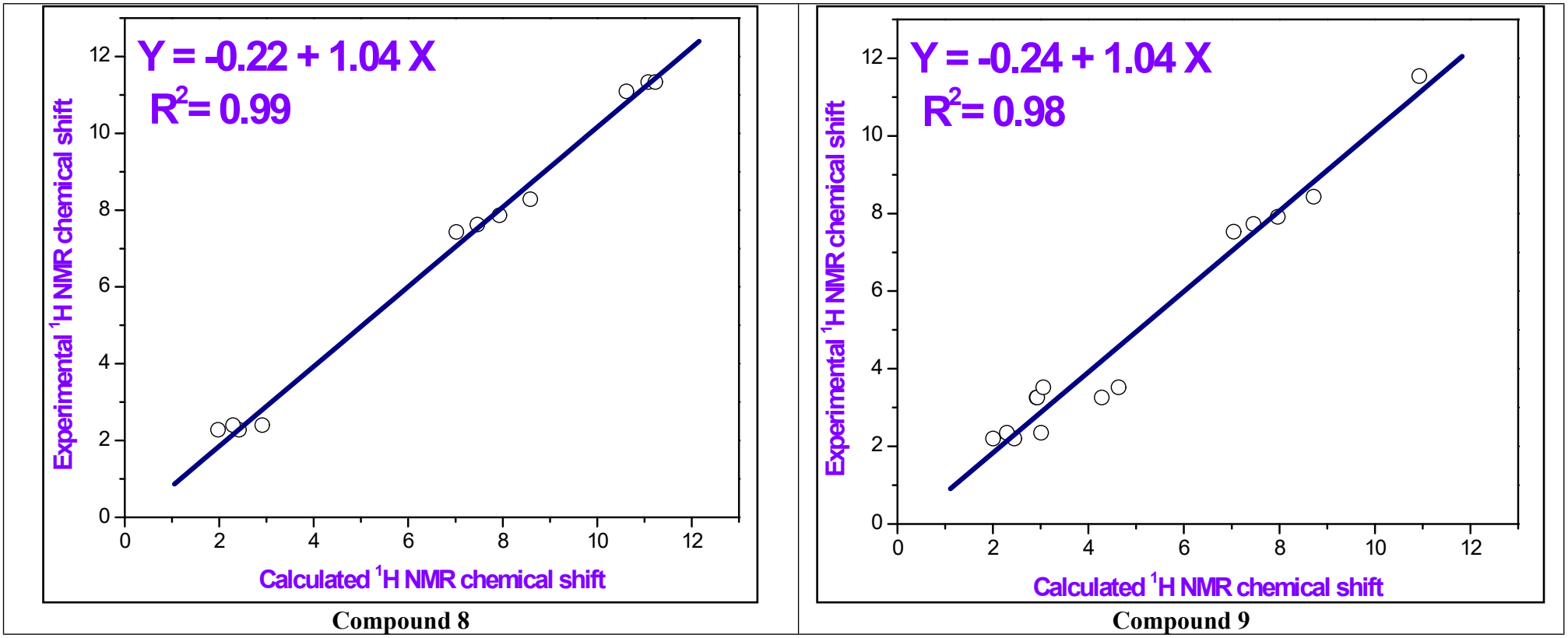

Fig. S9. The correlation relationships of the experimental *versus* calculated ^{1}H NMR chemical shifts of compounds **8** and **9**.

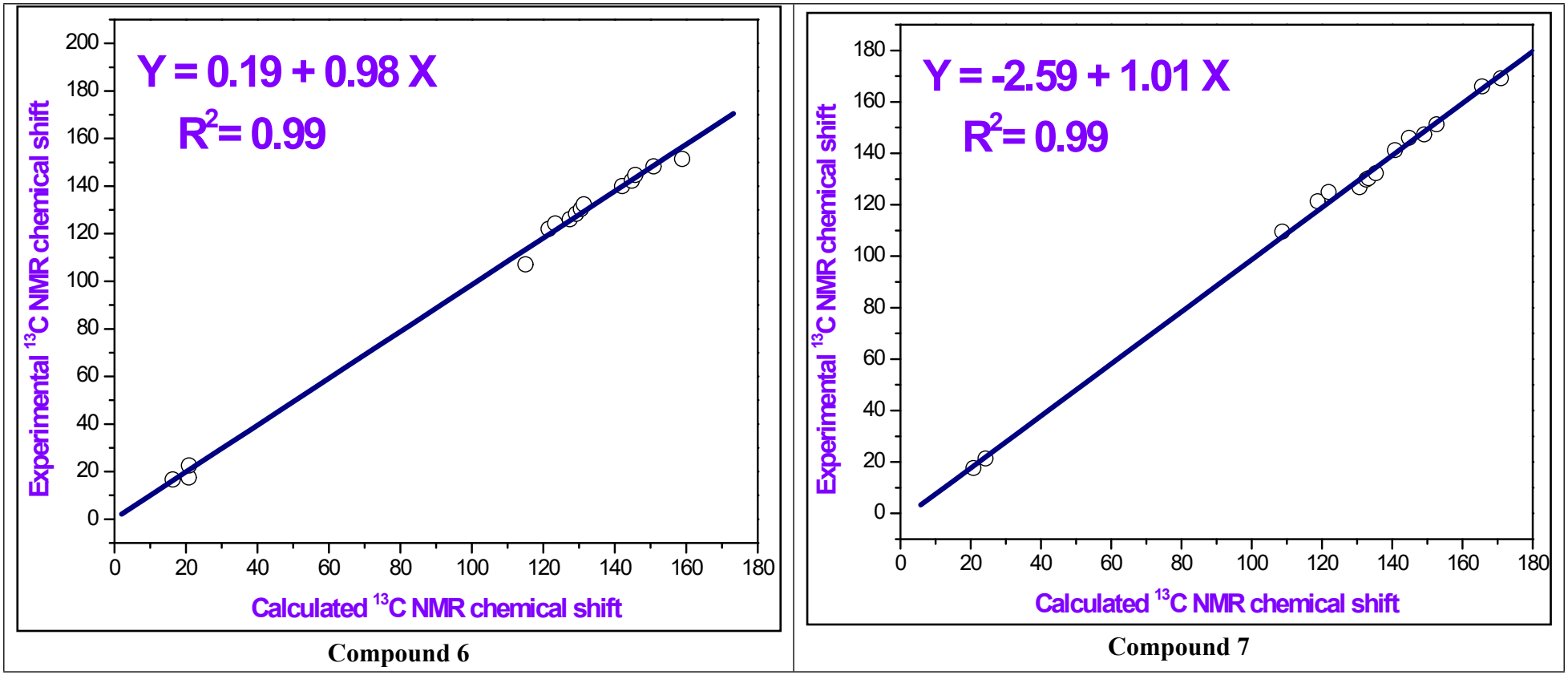

Fig. S10. The correlation relationships of the experimental *versus* calculated ^{13}C NMR chemical shifts of compounds **6** and **7**.

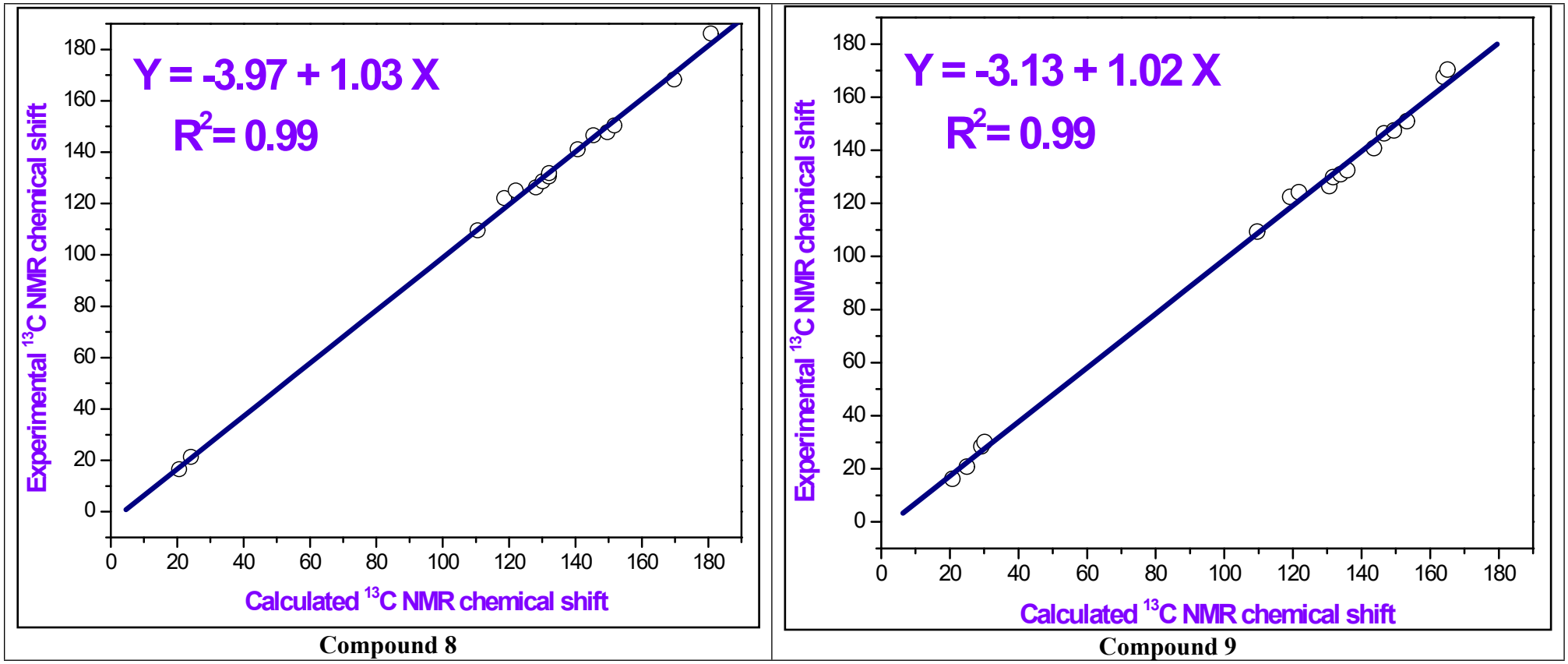

Fig. S11. The correlation relationships of the experimental *versus* calculated ^{13}C NMR chemical shifts of compounds **8** and **9**.

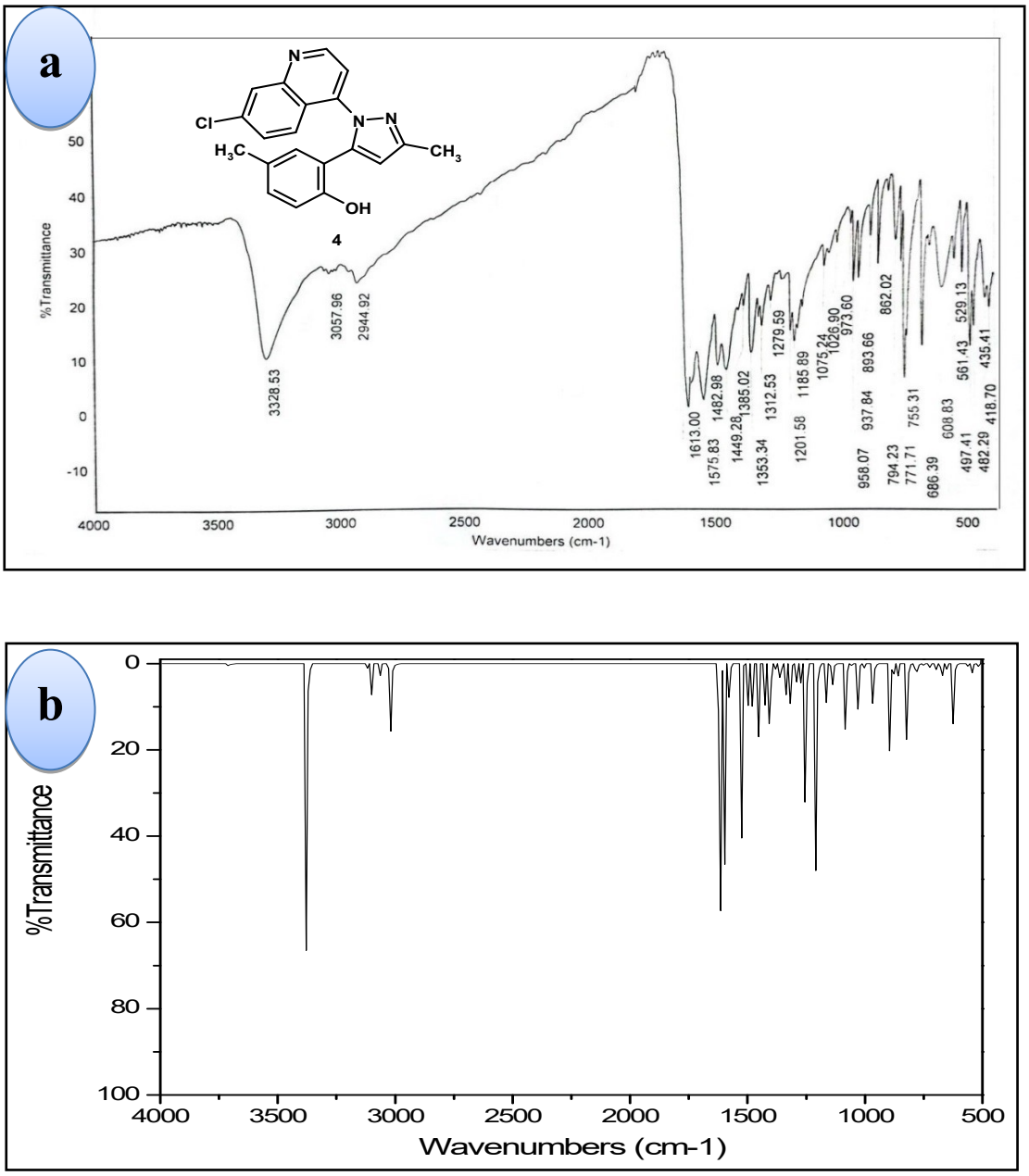

Fig. S12. (a) Experimental and (b) Calculated IR spectra of compound **4** at B3LYP/6-311++G(d,p).

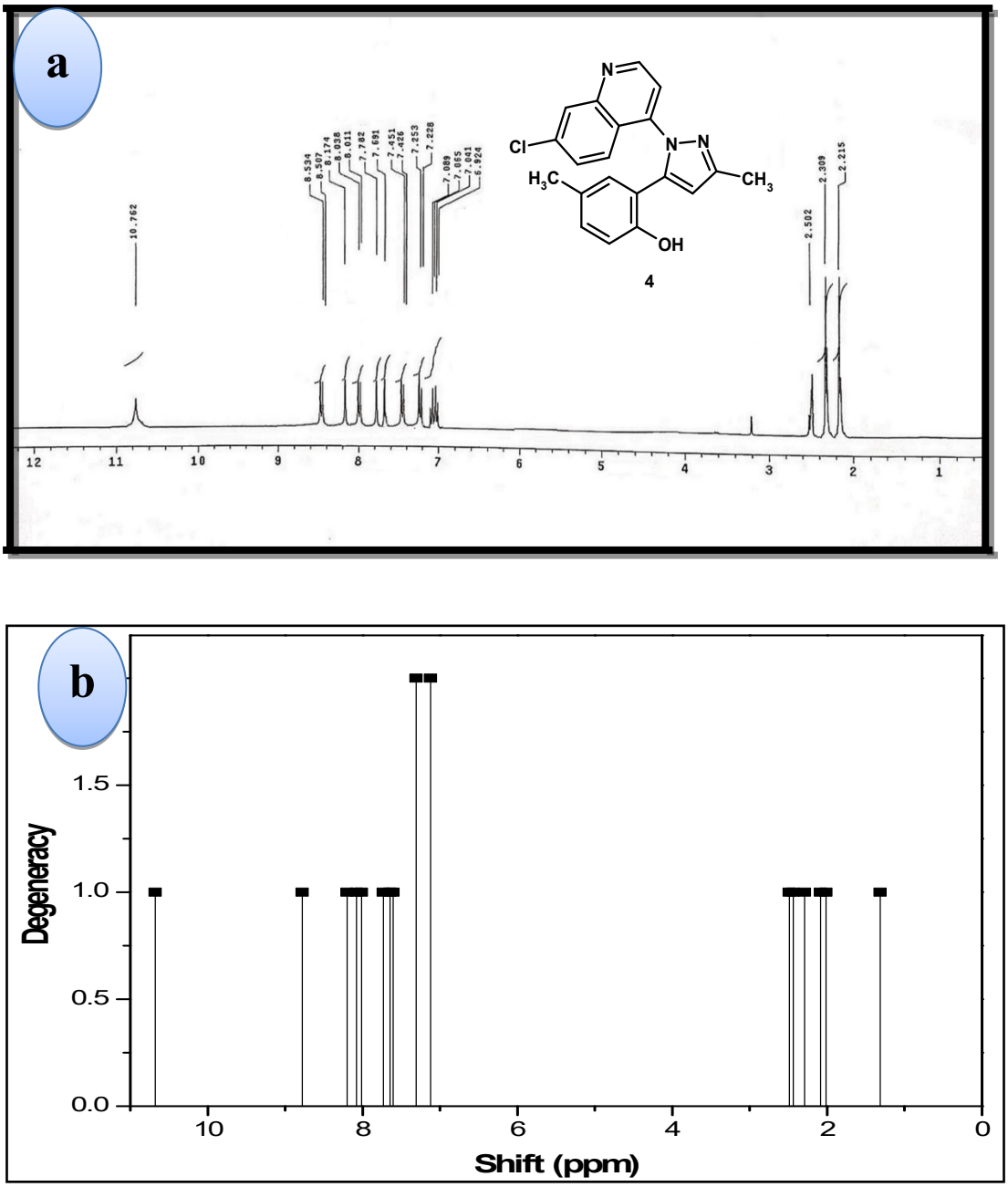

Fig. S13. (a) Experimental and (b) Calculated ^{1}H NMR spectra of compound **4** at B3LYP/6-311++G(d,p).

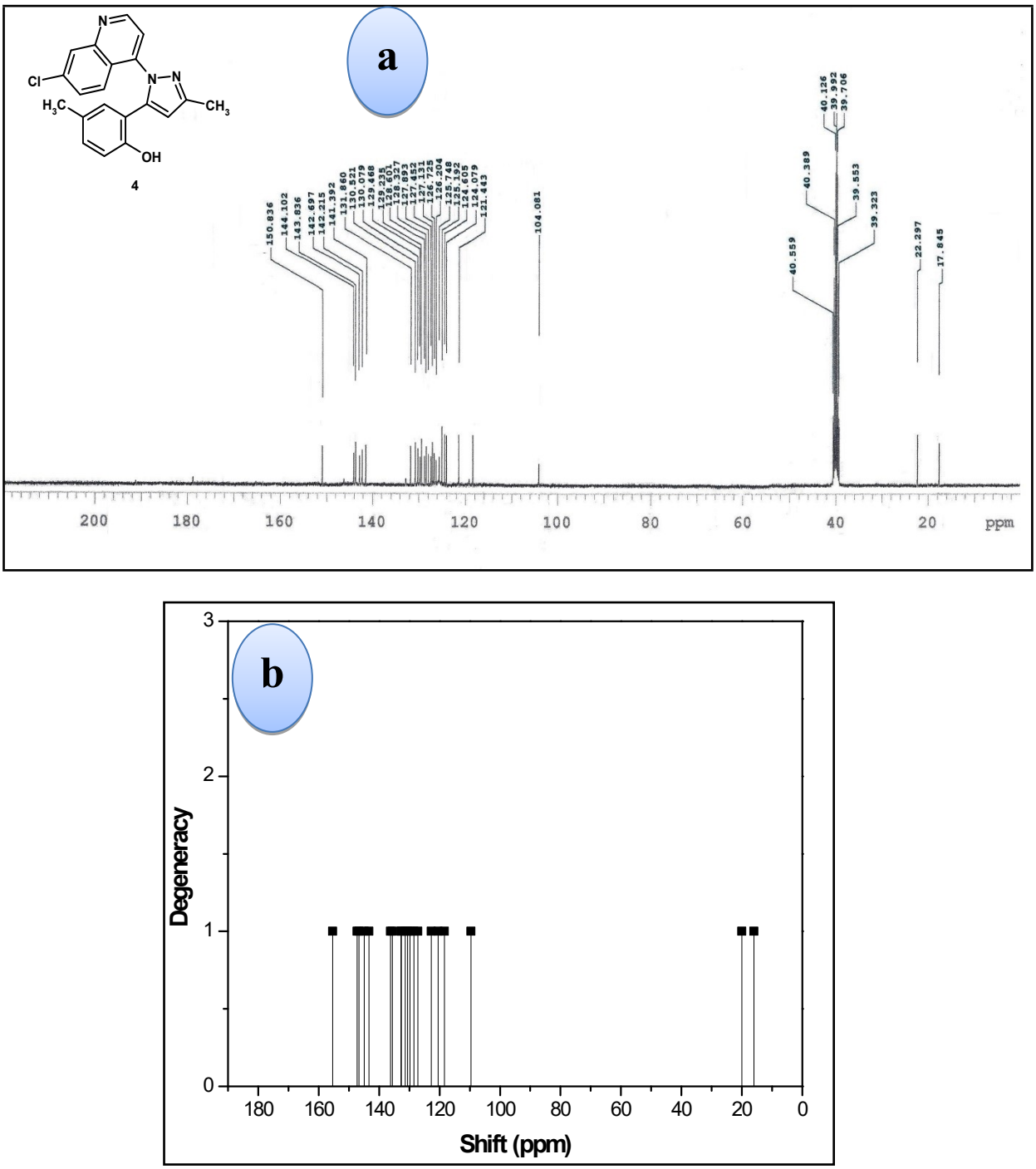

Fig. S14. (a) Experimental and (b) Calculated ^{13}C NMR spectra of compound **4** at B3LYP/6-311++G(d,p).

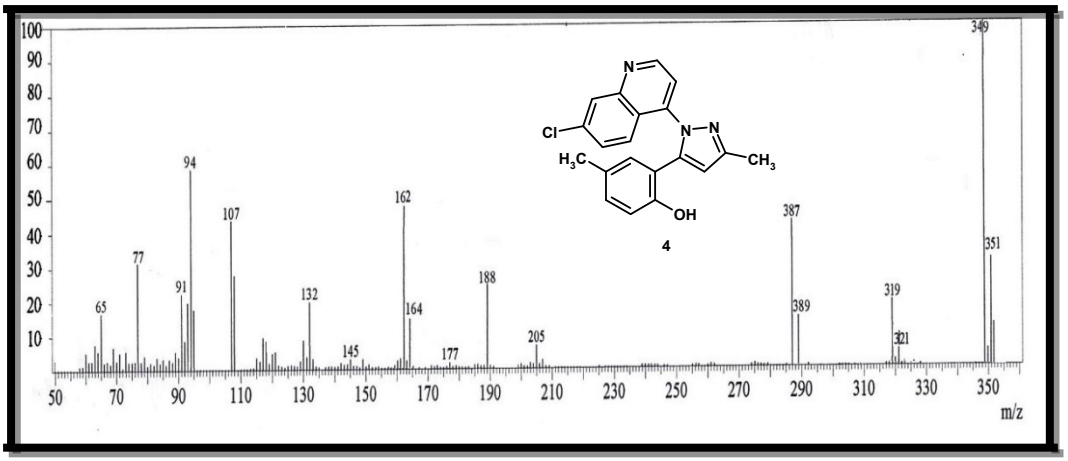

Fig. S15. Mass spectrum of compound **4**

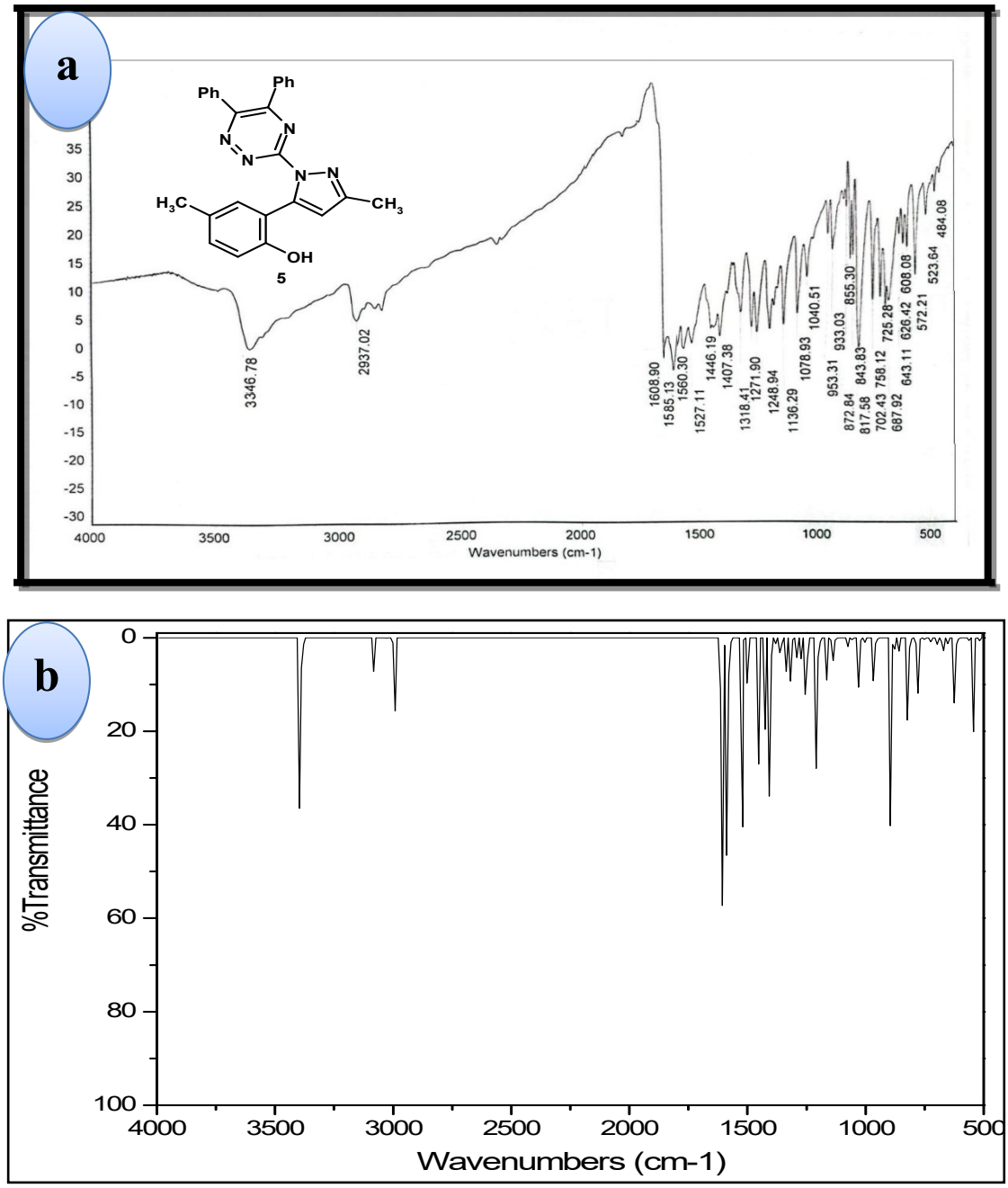

Fig. S16. (a) Experimental and (b) Calculated IR spectra of compound **5** at B3LYP/6-311++G(d,p).

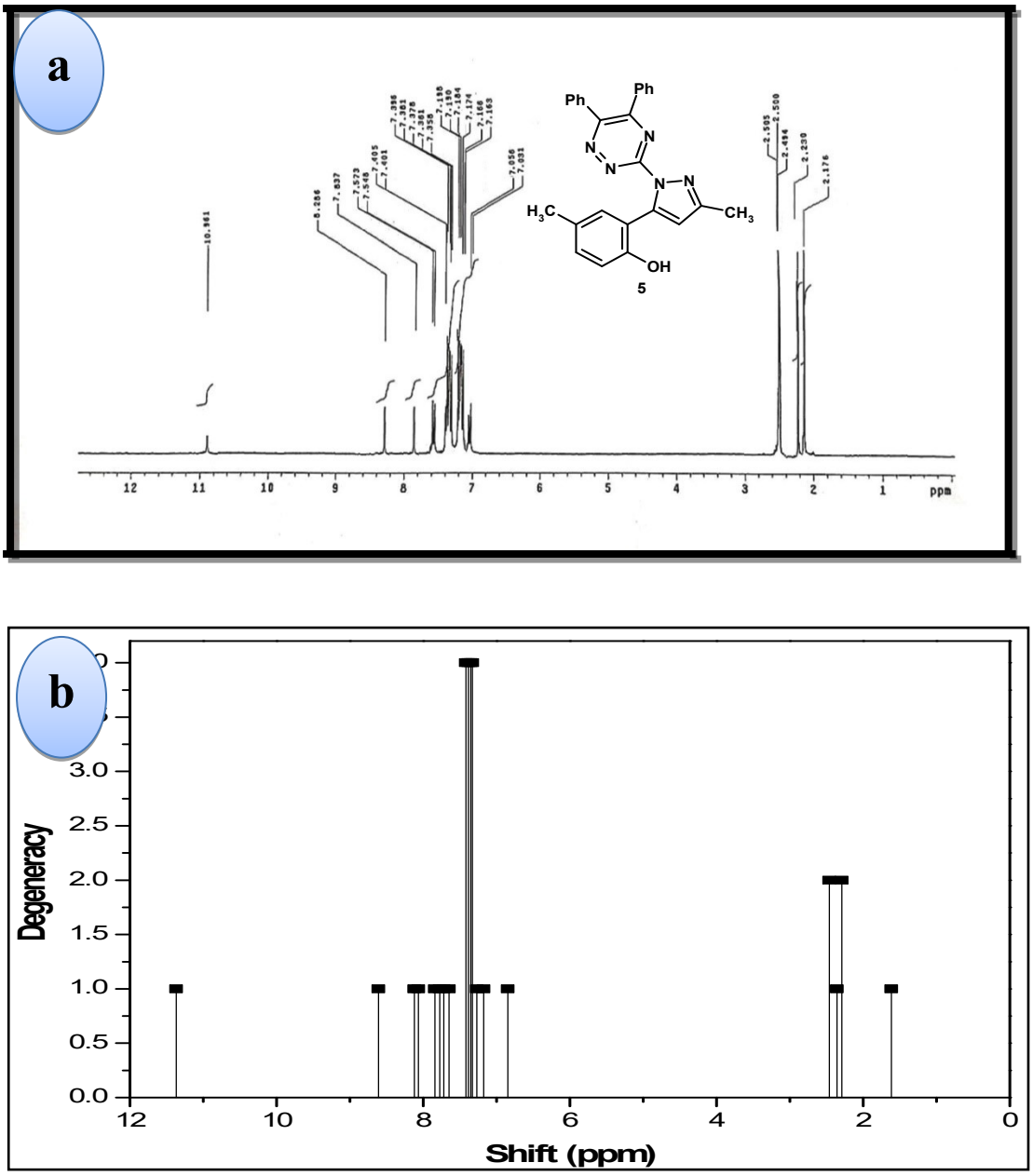

Fig. S17. (a) Experimental and (b) Calculated ^{1}H NMR spectra of compound **5** at B3LYP/6-311++G(d,p).

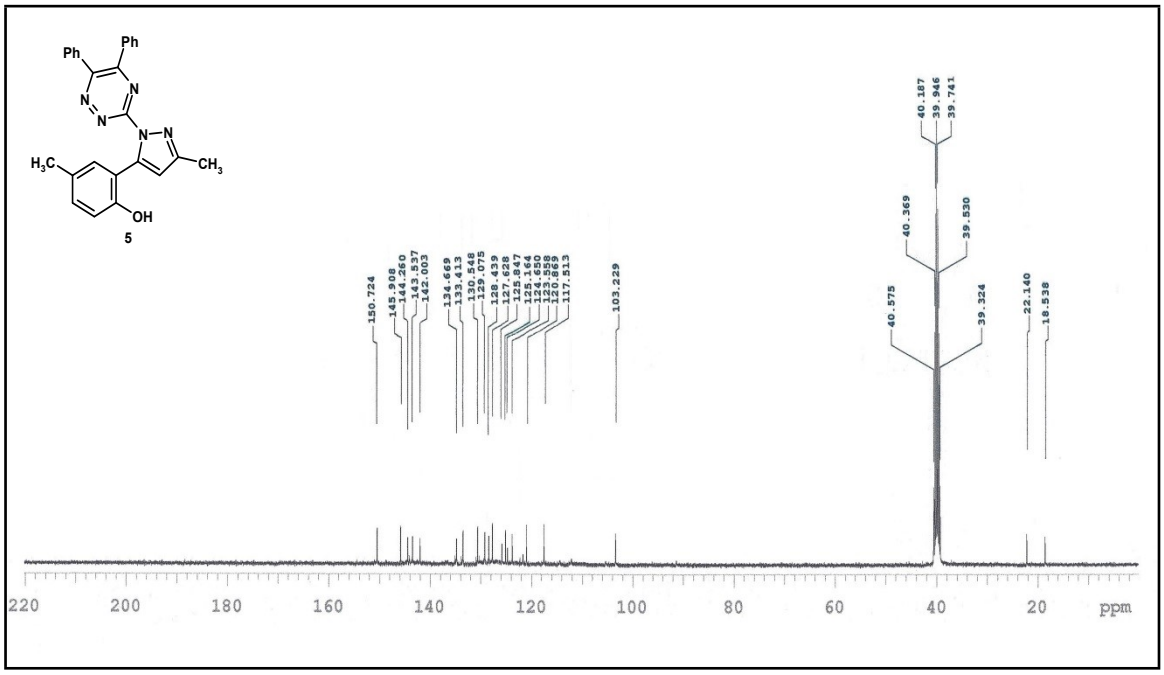

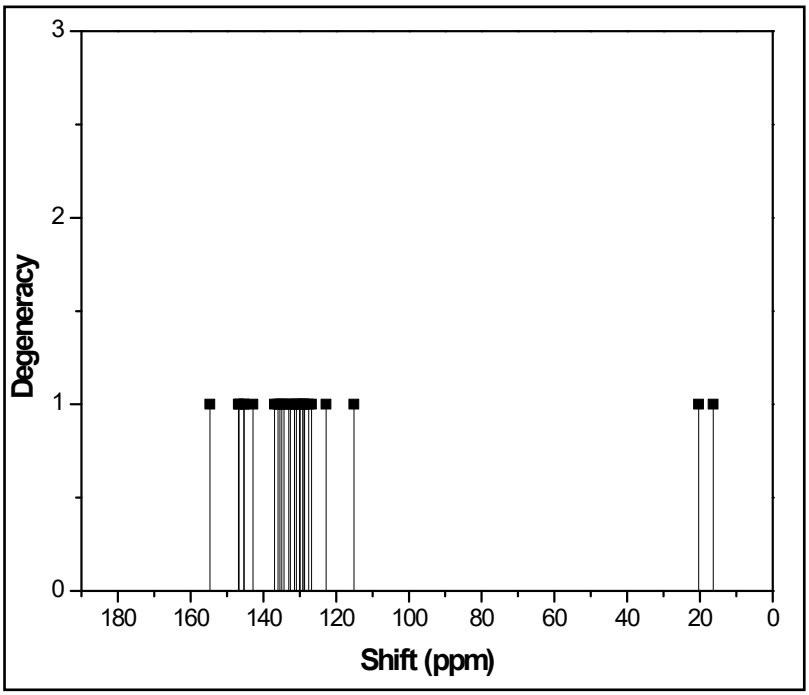

Fig. S18. (a) Experimental and (b) Calculated ^{13}C NMR spectra of compound **5** at B3LYP/6-311++G(d,p).

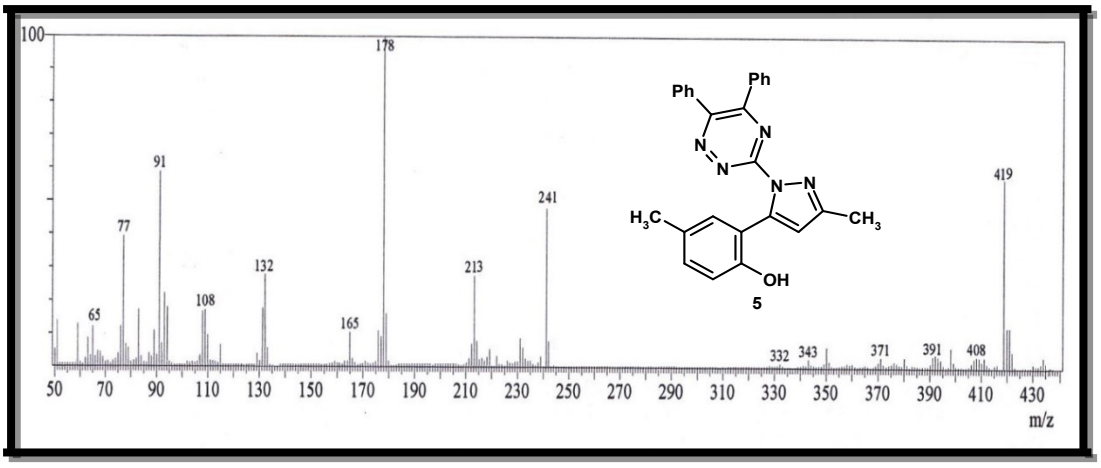

Fig. S19. Mass spectrum of compound **5**

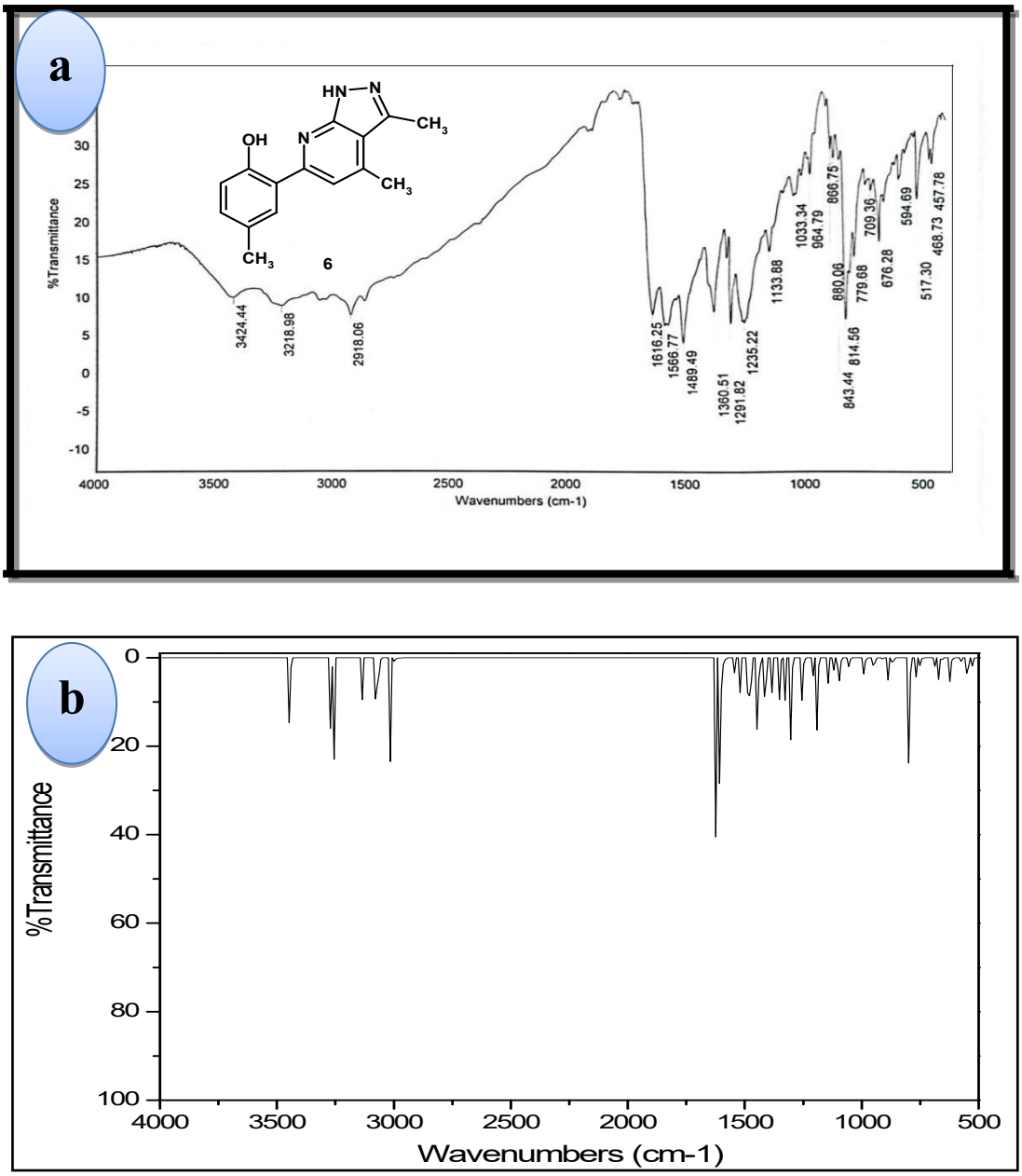

Fig. S20. (a) Experimental and (b) Calculated IR spectra of compound **6** at B3LYP/6-311++G(d,p).

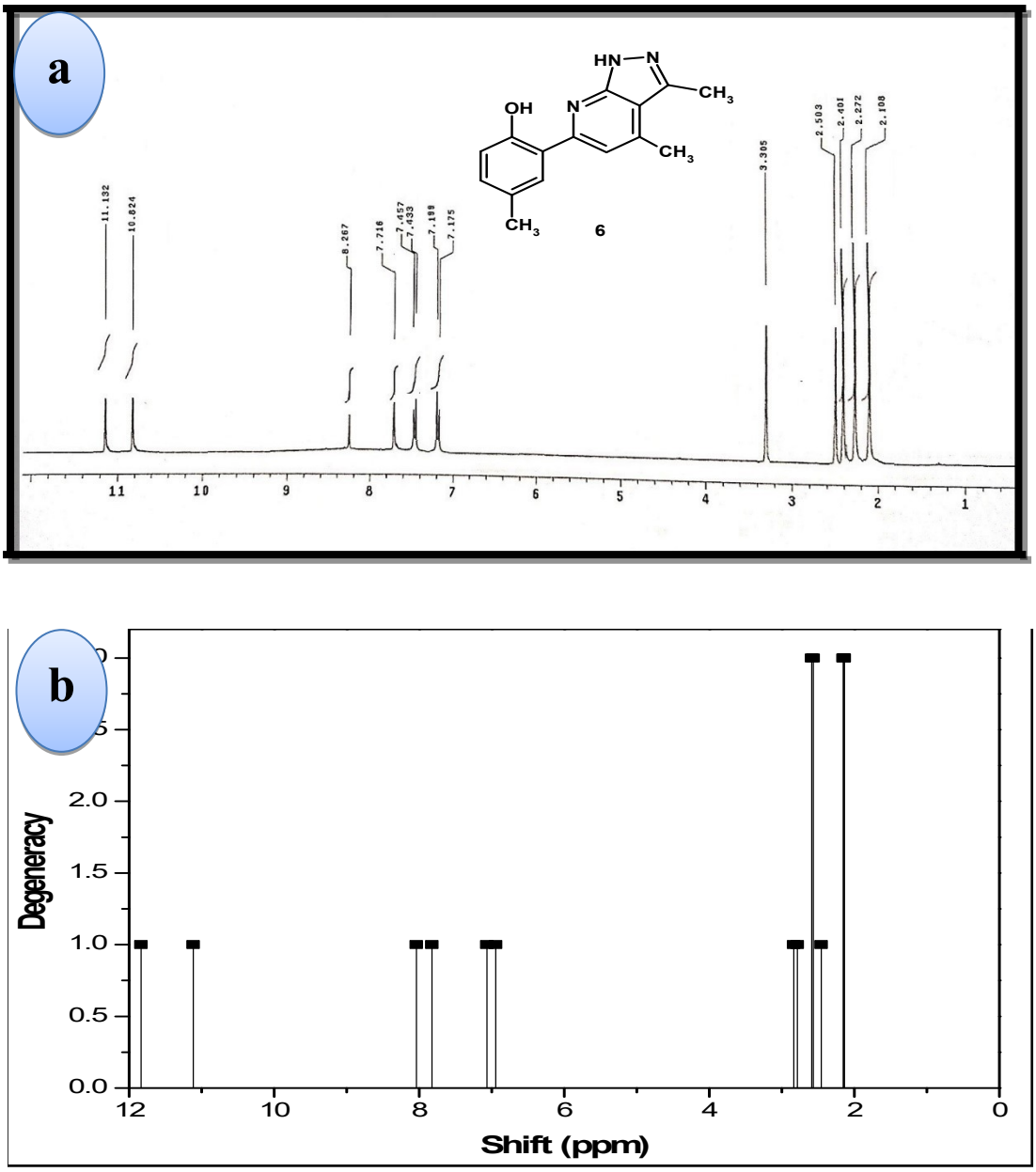

Fig. S21. (a) Experimental and (b) Calculated ^{1}H NMR spectra of compound **6** at B3LYP/6-311++G(d,p).

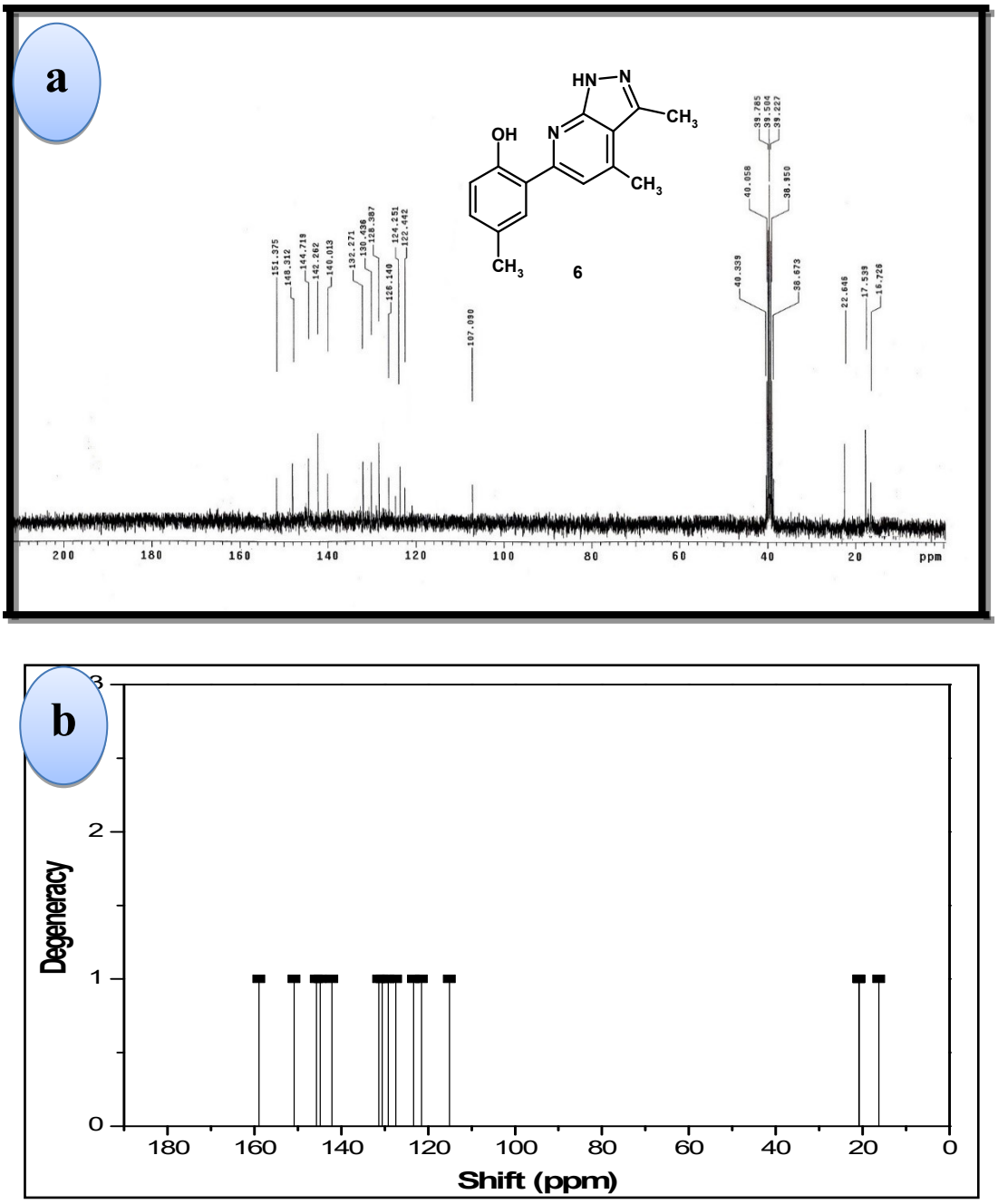

Fig. S22. (a) Experimental and (b) Calculated ^{13}C NMR spectra of compound **6** at B3LYP/6-311++G(d,p).

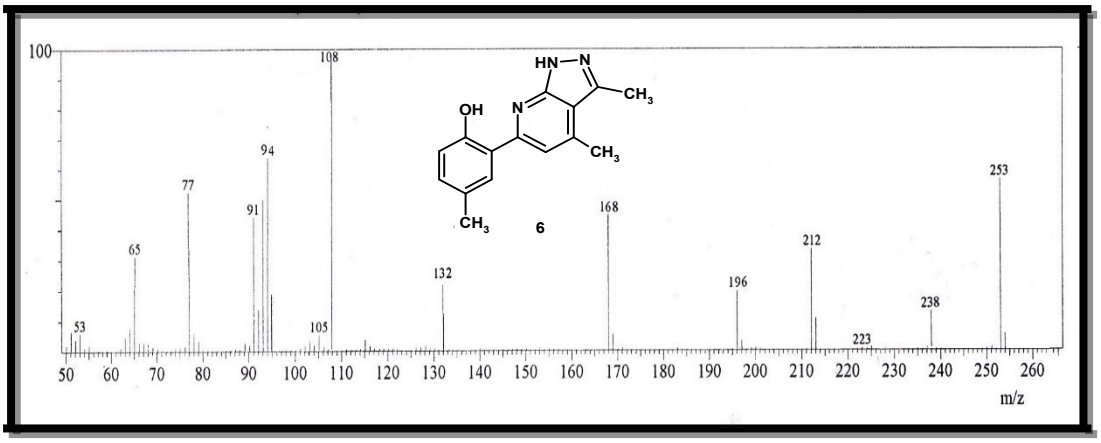

Fig. S23. Mass spectrum of compound **6**

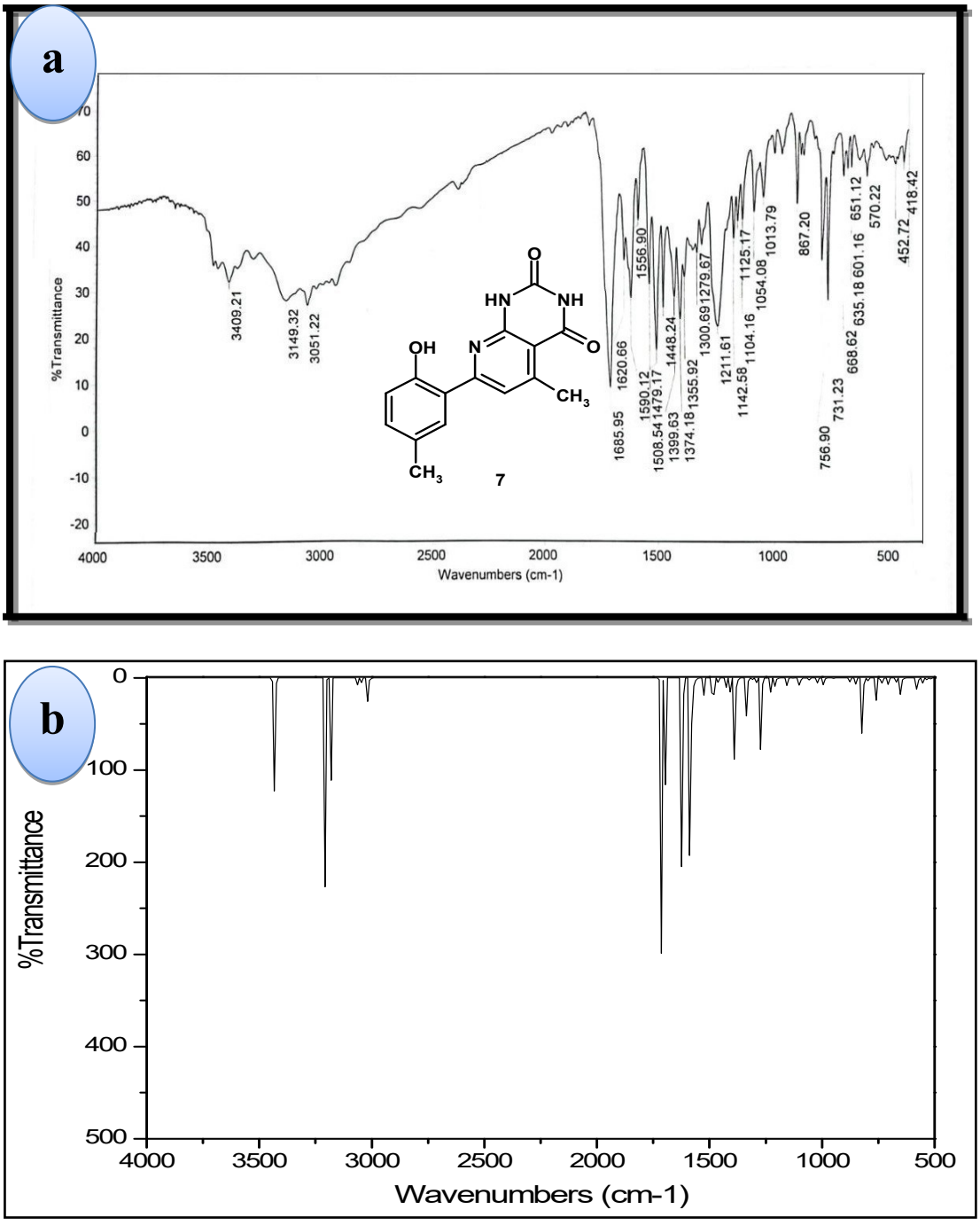

Fig. S24. (a) Experimental and (b) Calculated IR spectra of compound **7** at B3LYP/6-311++G(d,p).

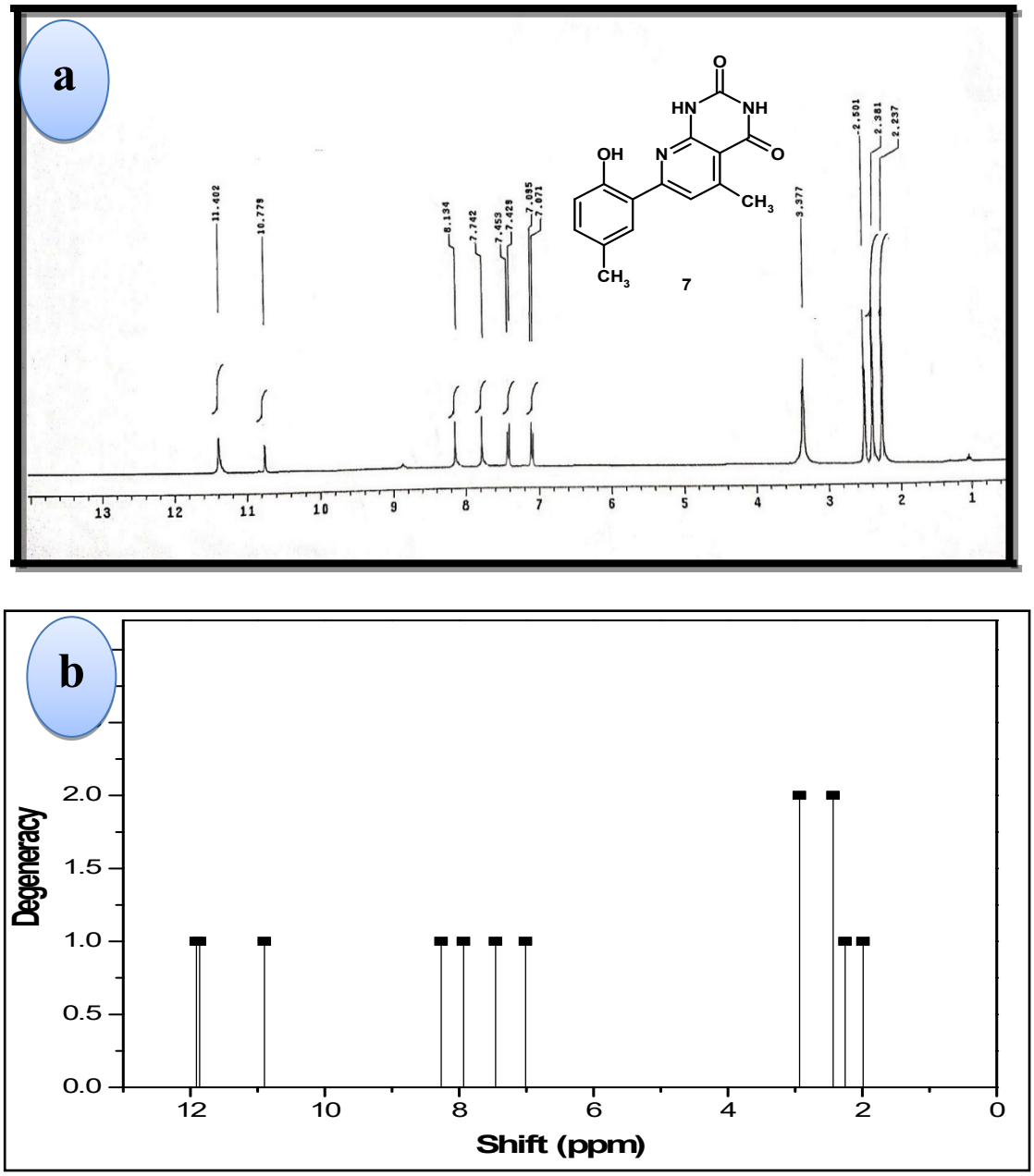

Fig. S25. (a) Experimental and (b) Calculated ^{1}H NMR spectra of compound **7** at B3LYP/6-311++G(d,p).

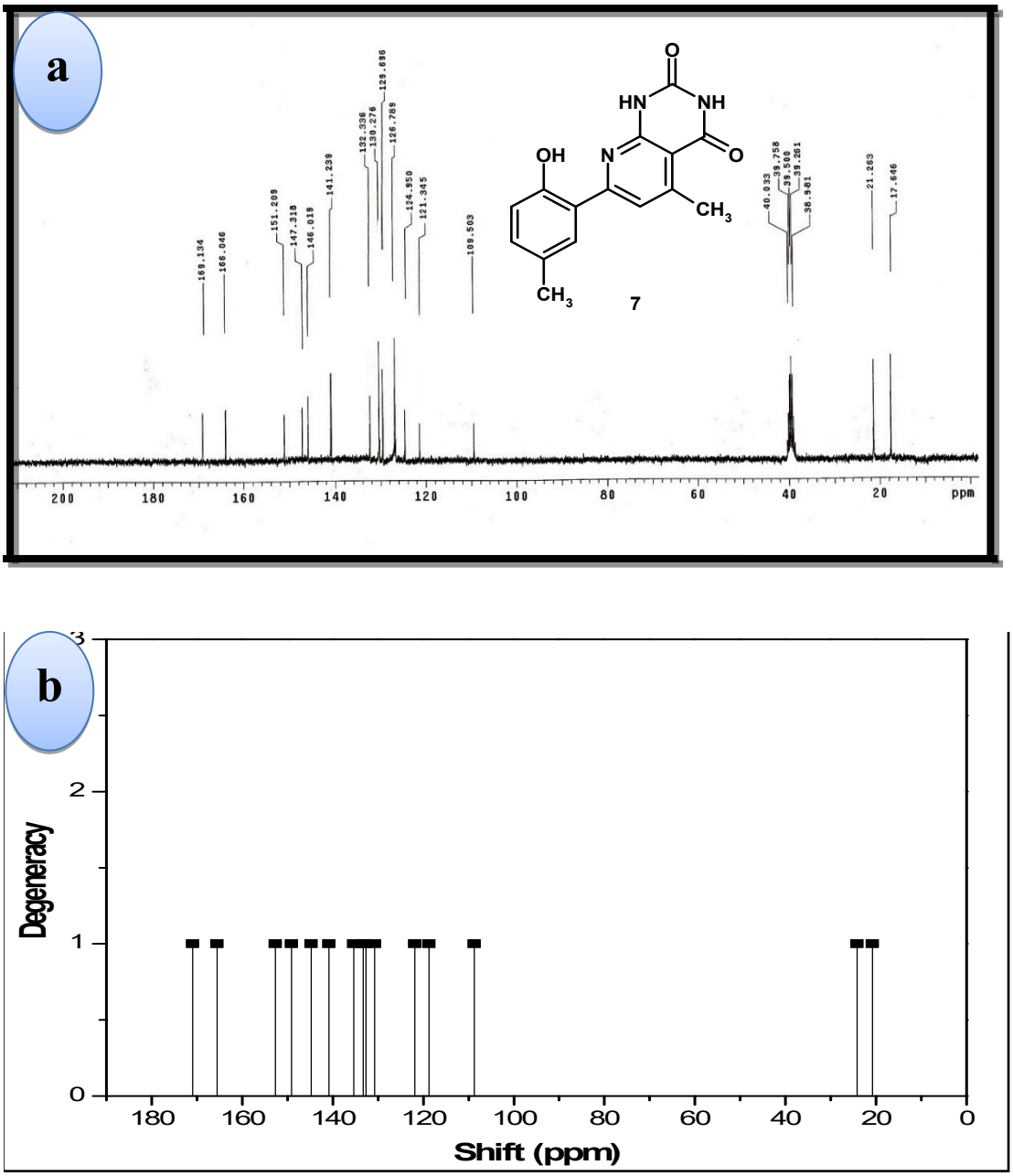

Fig. S26. Experimental and Calculated ^{13}C NMR spectra of compound **7** at B3LYP/6-311++G(d,p).

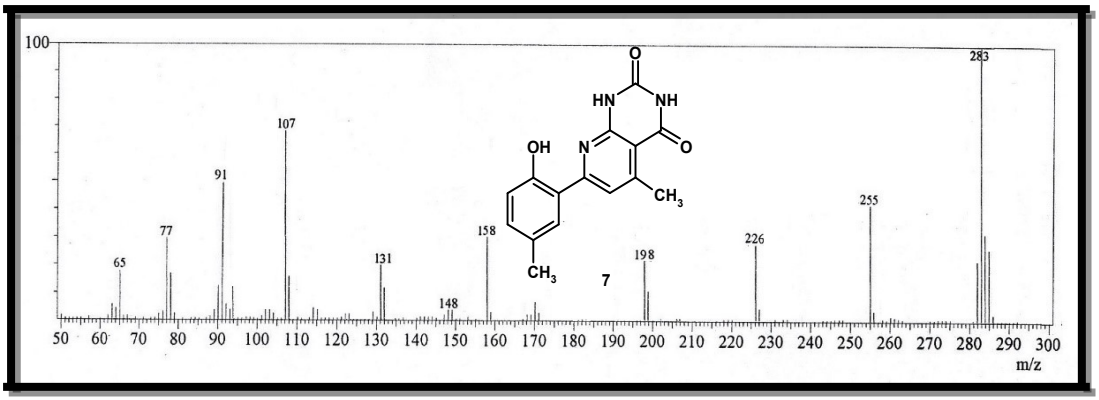

Fig. S27. Mass spectrum of compound **7**

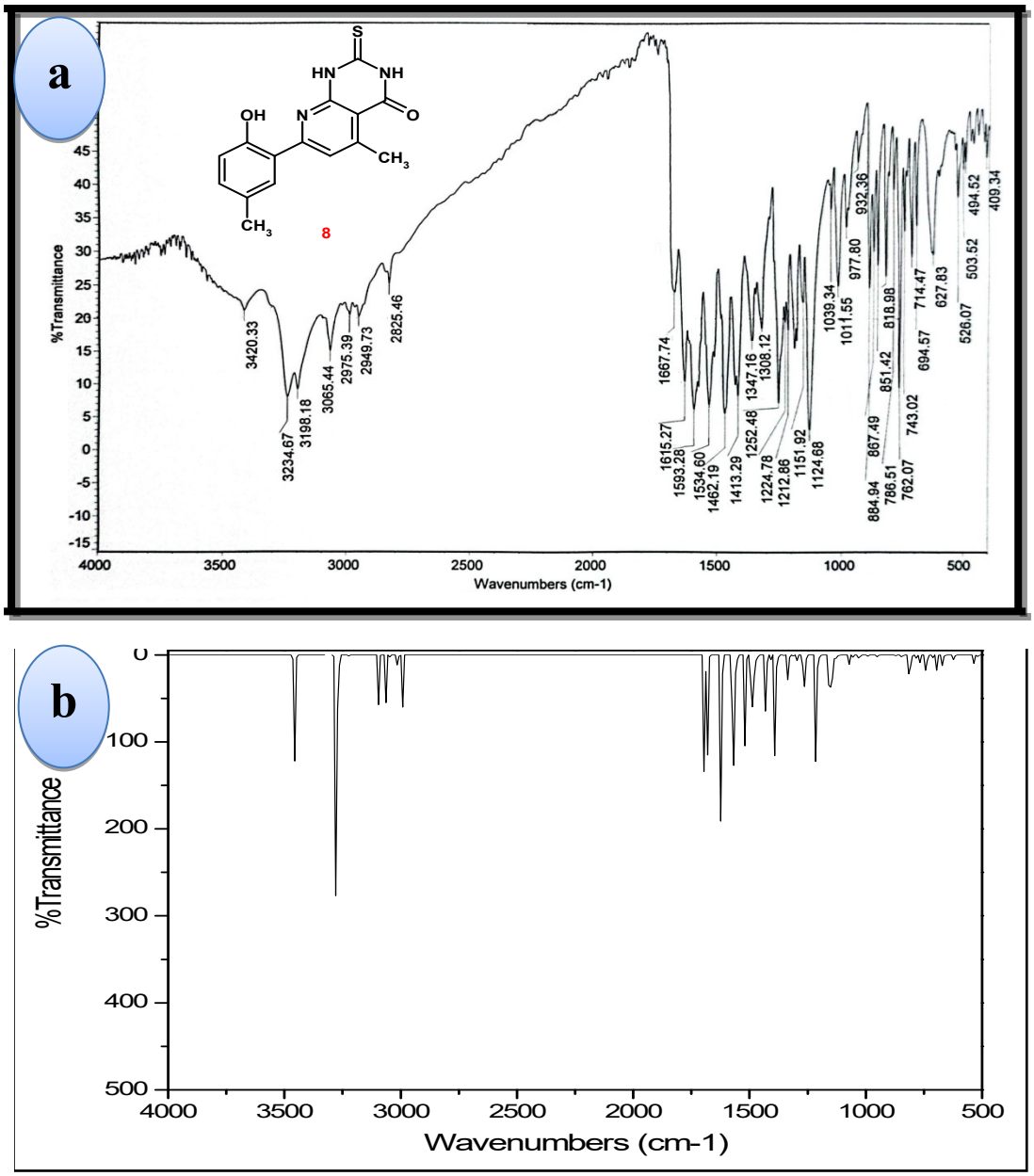

Fig. S28. (a) Experimental and (b) Calculated IR spectra of compound **8** at B3LYP/6-311++G(d,p).

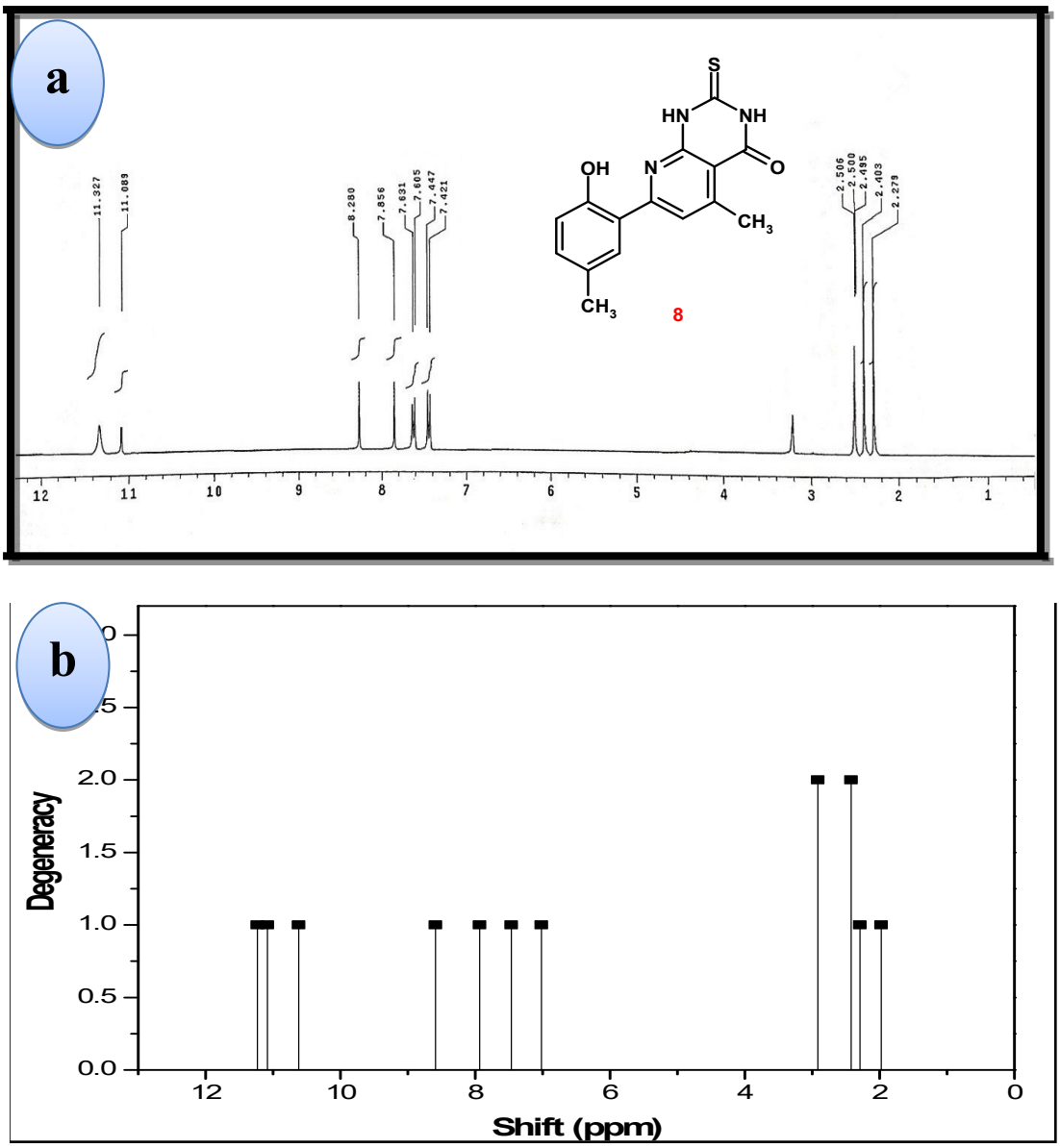

Fig. S29. (a) Experimental and (b) Calculated ^{1}H NMR spectra of compound **8** at B3LYP/6-311++G(d,p).

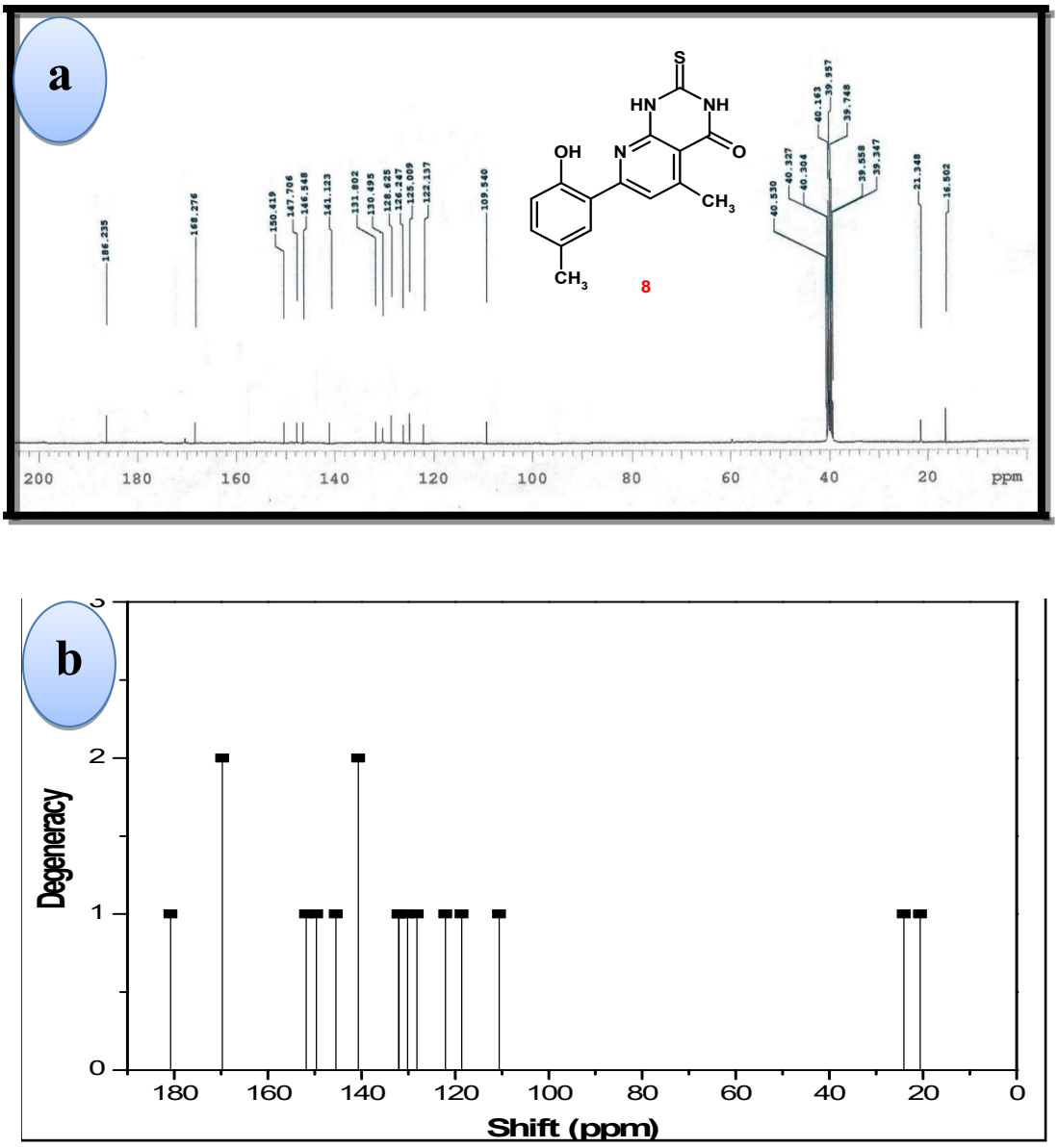

Fig. S30. Experimental and Calculated ^{13}C NMR spectra of compound **8** at B3LYP/6-311++G(d,p).

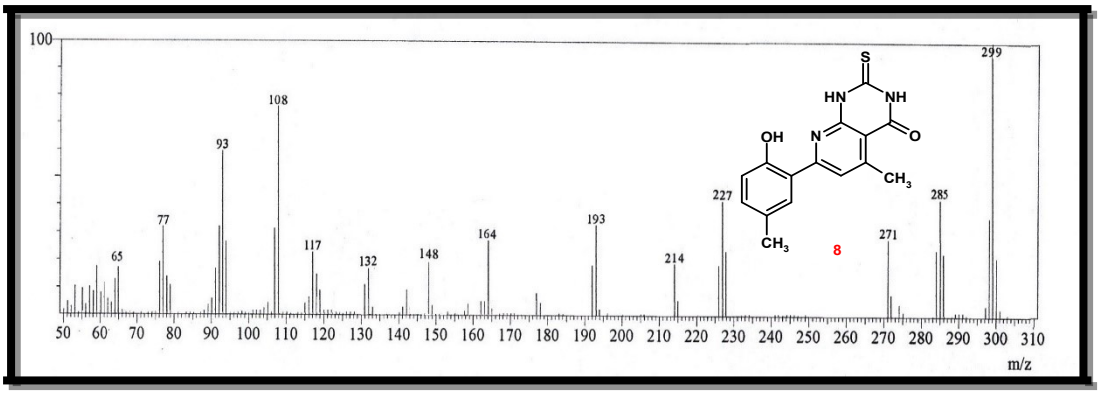

Fig. S31. Mass spectrum of compound **8**

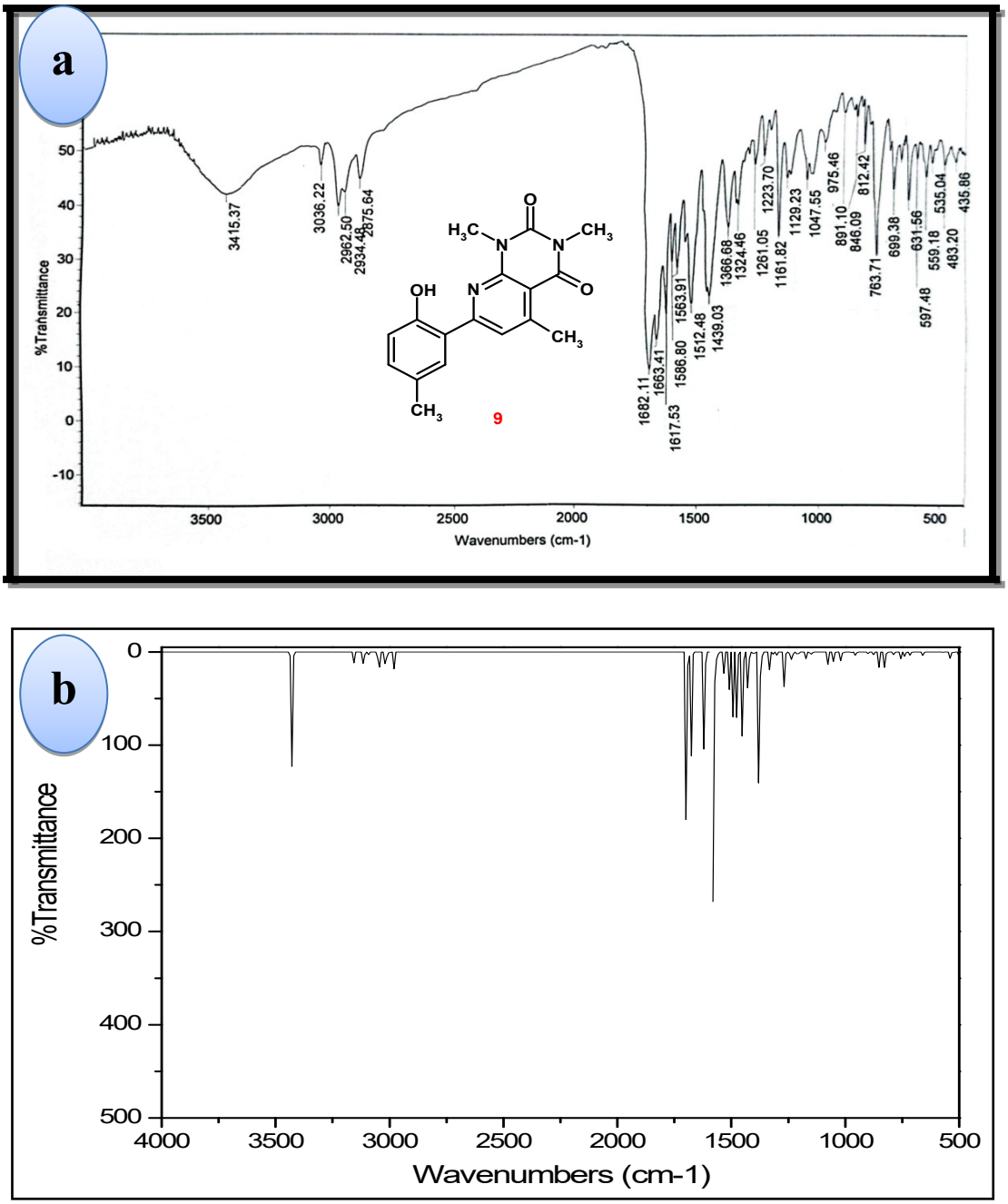

Fig. S32. (a) Experimental and (b) Calculated IR spectra of compound **9** at B3LYP/6-311++G(d,p).

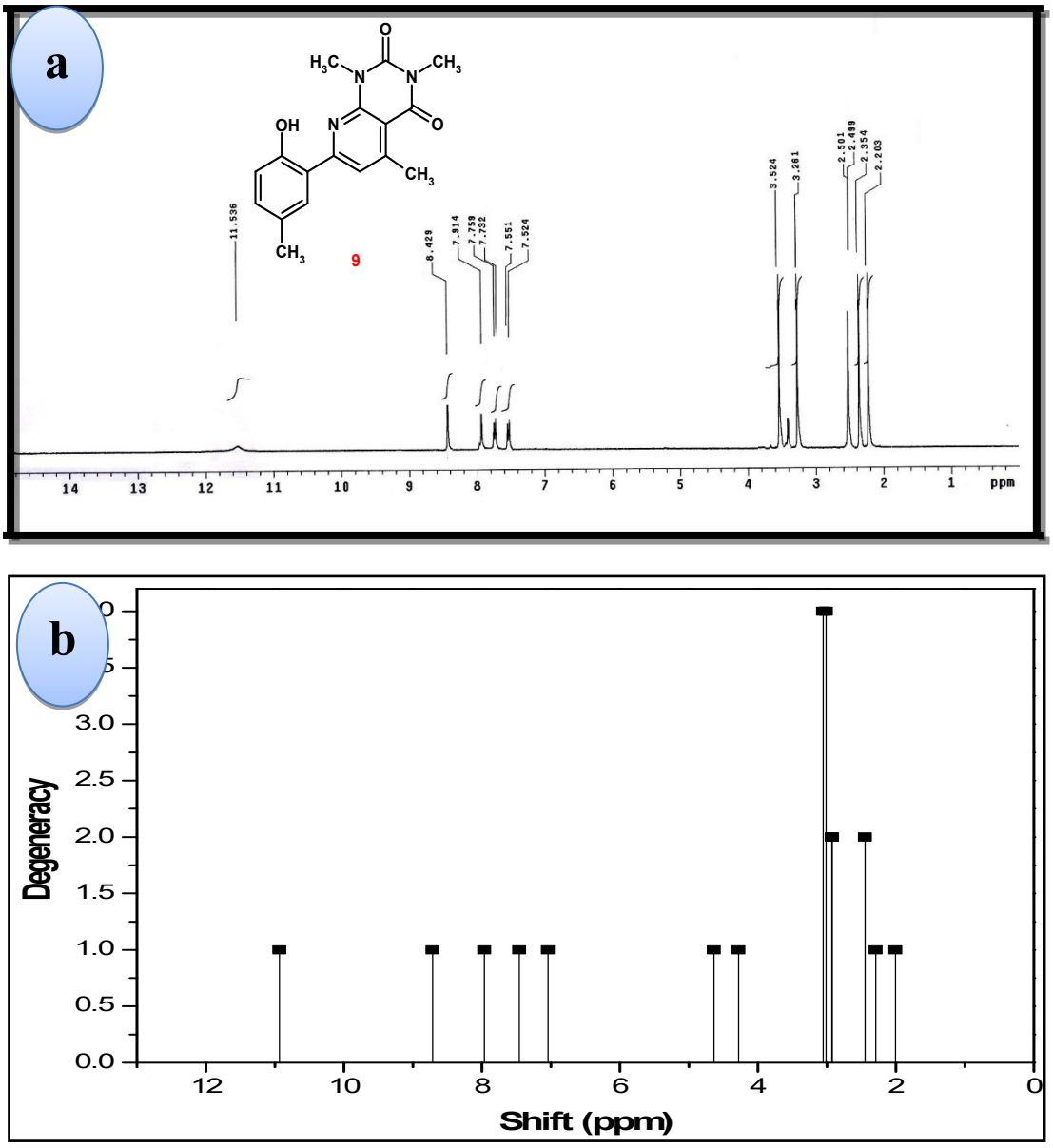

Fig. S33. (a) Experimental and (b) Calculated ^{1}H NMR spectra of compound **9** at B3LYP/6-311++G(d,p).

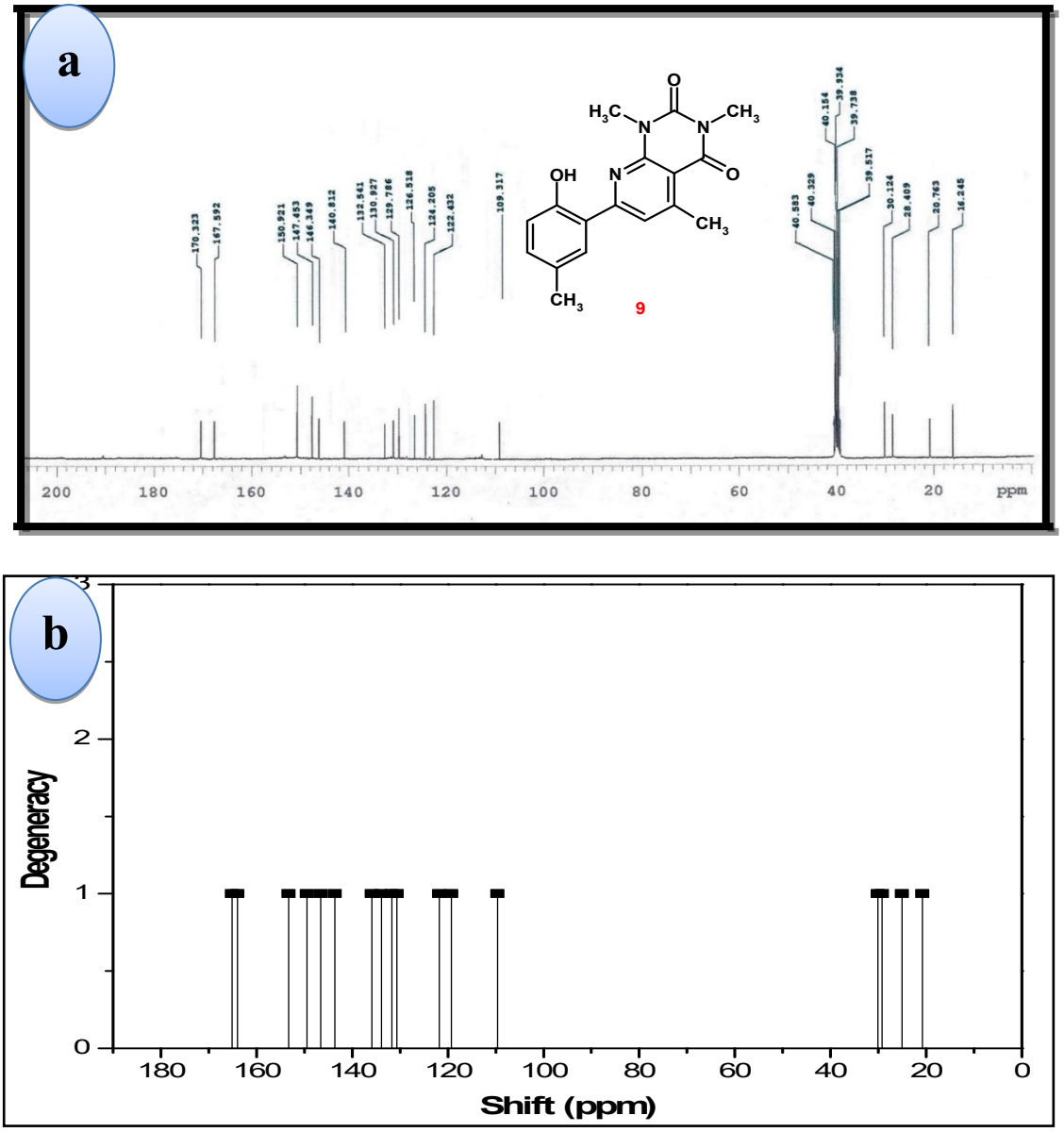

Fig. S34. Experimental and Calculated ^{13}C NMR spectra of compound **7** at B3LYP/6-311++G(d,p).

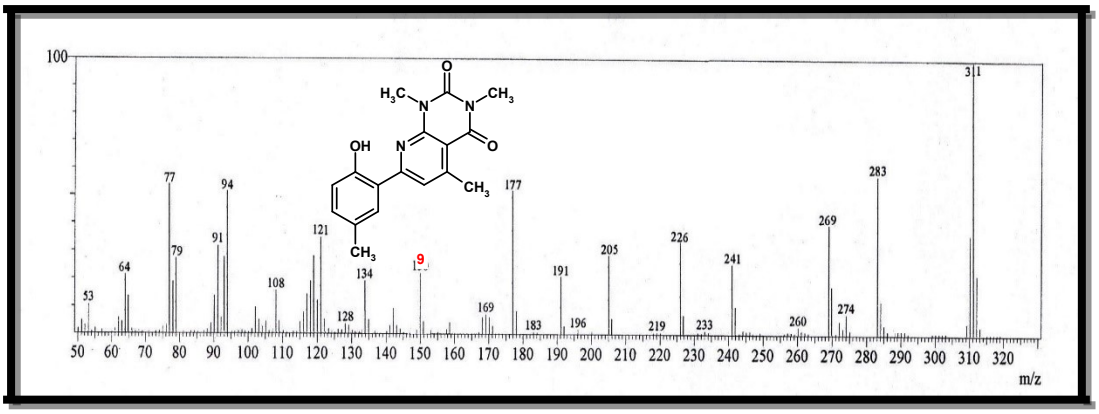

Fig. S35. Mass spectrum of compound **9**

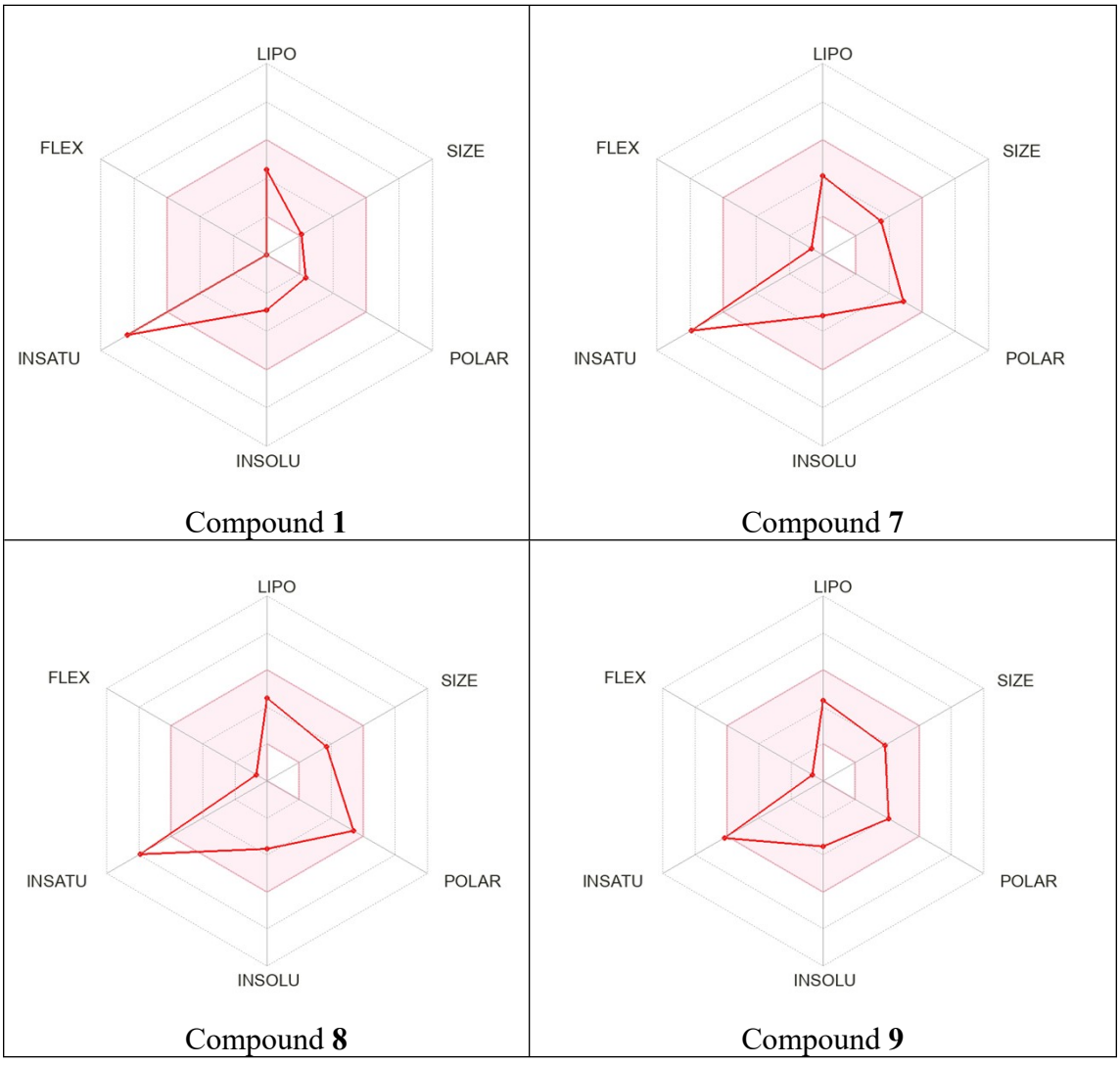

Fig. S36. The bioavailability radars of compounds **1** and **7-9**

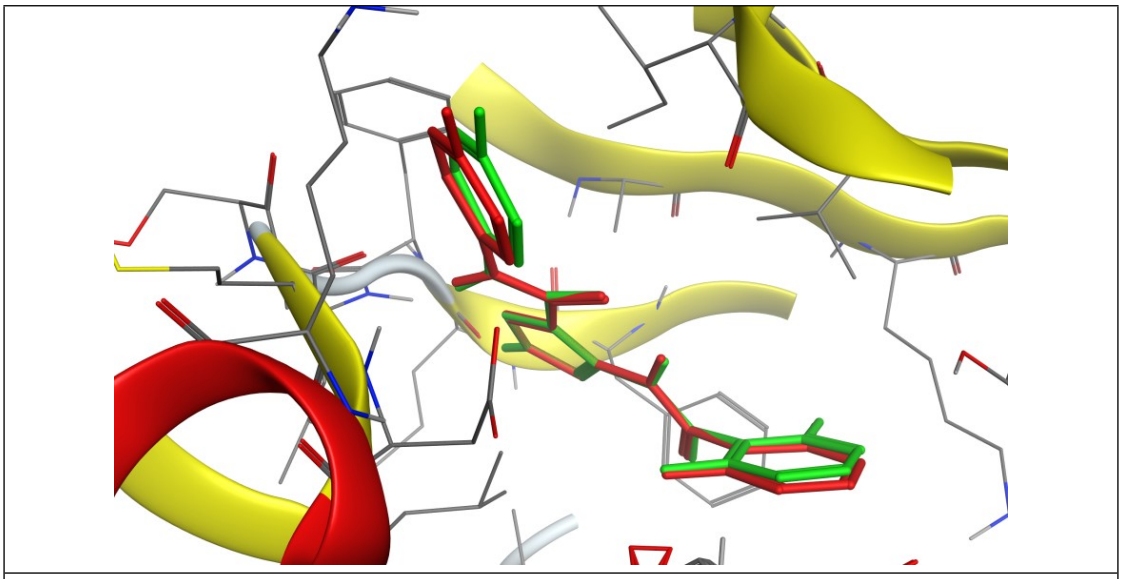

Fig. S37. 3D representation of the superimposition of the co-crystallized (red) and the redocking pose (green) of the ([(2,6-difluorophenyl)carbonyl]amino)-N-(4-fluorophenyl)-1H-pyrazole-3-carboxamide ligand in target protein (pdb ID: 4Y72).

Compound	2D
4	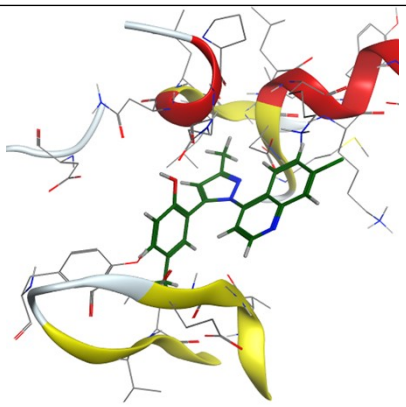
6	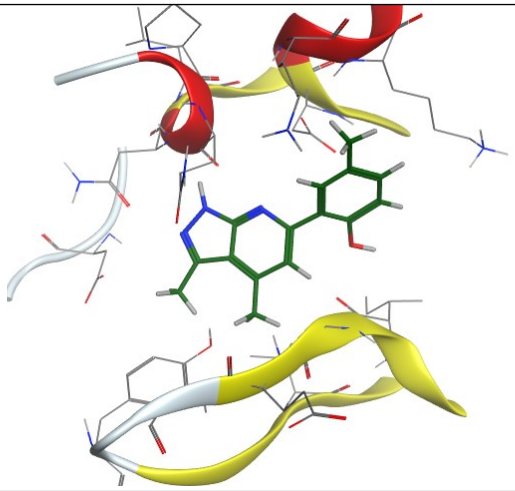
9	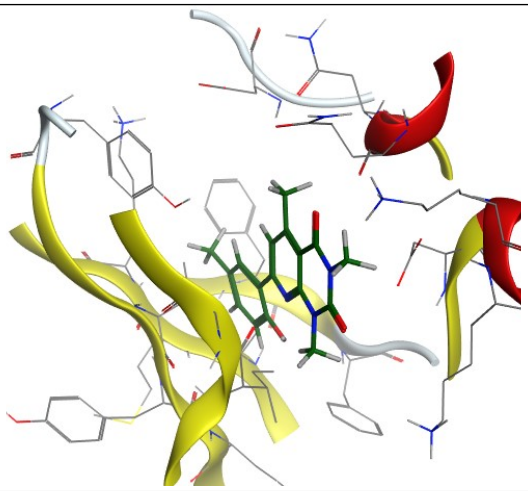

Fig. S38. 2D representation of the hydrogen bonding between the studied compounds (**4**, **6**, **9**) with the amino acids residues of the target protein (PDB ID: 4Y72).

Table S1. Various interactions between the studied compounds **4**, **6** and **9** with the amino acids residues of the target protein (pdb ID: 4Y72).

Compound 4 (Binding energy -8.10 kcal/mol)			**Compound 6** (Binding energy -7.80 kcal/mol)		
Receptor	Distance	Interaction Type	Receptor	Distance	Interaction Type
ALA31	2.90	Pi-Sigma	ASN133	2.65	H-Bond
LYS89	3.83	Alkyl	ASP86	2.59	Pi-Anion
ILE10	4.29	Pi-Alkyl	VAL18	4.85	Alkyl
ALA31	3.71	Pi-Alkyl	LYS88	3.70	Alkyl
LYS33	4.39	Pi-Alkyl	LYS89	4.47	Alkyl
LYS20	5.28	Pi-Alkyl	TYR15	5.02	Pi-Alkyl
			LYS89	4.73	Pi-Alkyl
Compound 9 (Binding energy -8.40 kcal/mol)					
ILE10	2.18	H-Bond			
ILE10	2.14	H-Bond			
ASP86	2.86	H-Bond			
ASP86	2.78	H-Bond			
ASP86	3.31	Pi-Anion			
VAL18	4.63	Amide-Pi Stacked			
ALA31	4.43	Alkyl			
LYS88	4.82	Alkyl			
VAL18	2.91	Alkyl			
LYS33	3.78	Alkyl			
PHE80	4.96	Pi-Alkyl			
ILE10	5.38	Pi-Alkyl			
VAL18	4.95	Pi-Alkyl			
ALA31	3.83	Pi-Alkyl			